where the t_i designate the odd integers associated with the states. The use of (B4) and (21)–(24) reduces the number of independent spectral densities associated with the pair of Kramers doublets to just six. These are

$$T_{13,31}{}^{+}(\omega)=T_{24,42}{}^{+}(\omega)=\varphi(\omega)B_1/2\,, \tag{B5}$$

$$T_{14,41}{}^{+}(\omega)=T_{23,32}{}^{+}(\omega)=\varphi(\omega)B_2/2\,, \tag{B6}$$

$$T_{13,41}{}^{+}(\omega)=-[T_{24,32}{}^{+}(\omega)]^{*}=\varphi(\omega)C/2\,, \tag{B7}$$

$$T_{32,13}(\omega)=-[T_{41,24}{}^{+}(\omega)]^{*}=\varphi(\omega)D/2\,, \tag{B8}$$

$$T_{24,31}{}^{+}(\omega)=[T_{13,42}{}^{+}(\omega)]^{*}=\varphi(\omega)E/2\,, \tag{B9}$$

$$T_{23,41}{}^{+}(\omega)=[T_{14,32}{}^{+}(\omega)]^{*}=\varphi(\omega)F/2\,, \tag{B10}$$

where $\varphi(\omega)$ is a function that is $n(|\hbar\omega|)$ for positive arguments and $n(|\hbar\omega|)+1$ for negative arguments. Two other nonzero spectral densities are

$$T_{23,31}{}^{+}(\omega)=-T_{24,41}{}^{+}(\omega)\,, \tag{B11}$$

$$T_{41,13}{}^{+}(\omega)=-T_{42,23}{}^{+}(\omega)\,, \tag{B12}$$

but they enter the master equation so as to cancel.

PHYSICAL REVIEW VOLUME 178, NUMBER 2 10 FEBRUARY 1969

Electron-Paramagnetic-Resonance Study of Cr Ions and Exchange-Coupled Cr Ion Pairs in the BiI_3 Structure*

R. W. Bené†
Department of Electrical Engineering, Stanford University, Stanford, California 96128
(Received 6 June 1968)

This paper reports the results of an EPR study of Cr^{3+} single ions in BiI_3 and SbI_3, and exchange-coupled pairs of Cr^{3+} ions in BiI_3. The spectrum for Cr^{3+} single ions in BiI_3 can be fitted by the spin Hamiltonian $\mathcal{H}_S=g\beta\mathbf{H}\cdot\mathbf{S}+DS_z^2$, where $g=2.058$ and $D=-0.5$ kOe. The spin Hamiltonian for Cr^{3+} single ions in SbI_3 is given by $\mathcal{H}_S=g_{\parallel}\beta H_zS_z+g_{\perp}\beta(H_xS_x+H_yS_y)+DS_z^2$, where $g_{\parallel}=2.078$, $g_{\perp}=2.088$, and $D=+3.85$ kOe. The spectrum for exchange-coupled intralayer pairs of Cr^{3+} ions in BiI_3 can be fitted by a spin Hamiltonian which has the terms $J\mathbf{S}_1\cdot\mathbf{S}_2+\frac{3}{2}J_zS_{1z}S_{2z}+\frac{1}{4}K[S_1{}^{+}S_2{}^{+}+S_1{}^{-}S_2{}^{-}]$ in addition to the single-ion terms for each Cr^{3+} ion. In the above expression J is negative, J_z+34 kOe, and $K=2.0$ kOe. Two of the results are rather unusual: a g value greater than 2, and an anisotropic exchange parameter about $\frac{1}{5}$ the isotropic exchange parameter. Explanations which involve the quite high covalent bonding and the extremely large spin-orbit constant on the halogens are given for both unusual parameters. The relevance of the EPR results to the magnetic anisotropy in the chromium trihalides is discussed. Also observed and included in this paper is the Cr^{2+} single-ion spectrum of BiI_3: Cr. The spin Hamiltonian for the Cr^{2+} transitions is given by $\mathcal{H}_S=g\beta\mathbf{H}\cdot\mathbf{S}+DS_z^2+E(S_x^2-S_y^2)$, where $g=1.98$, $D=6.9$ kOe, and $E=1.6$ kOe.

I. INTRODUCTION TO THE CHROMIUM TRIHALIDES AND THE ISOMORPHIC SERIES BiI_3, SbI_3, AND AsI_3

THE chromium trihalides ($CrCl_3$, $CrBr_3$, and CrI_3) appear to be an isomorphic[1,2] series of compounds with very interesting magnetic properties. $CrCl_3$ is an antiferromagnet with a transition temperature of 16.8°K. The spins lie in the plane perpendicular to the three-fold c axis. $CrBr_3$ and CrI_3 are ferromagnets with the spins lying along the c axis and with transition temperatures of 32.5 and 68°K, respectively. The site symmetry at the Cr site is C_3 and the space group is $R\bar{3}$. If an external field of a few kOe is applied, $CrCl_3$ also becomes ferromagnetic and almost isotropic.[3] The anistropy constants in $CrBr_3$ and CrI_3 are given at 1.5°K as -6.86 [4] and -28.6 kOe,[5] respectively. The chromium trihalides thus display quite a diverse set of macroscopic magnetic parameters, considering that they are isostructural and have lattice constants increasing by about 6–10% going from $CrCl_3$ to $CrBr_3$, and from $CrBr_3$ to CrI_3. In order to better understand these macroscopic parameters it is necessary to know more about the more basic interactions of a single magnetic Cr^{3+} ion with the nonmagnetic part of the lattice and of one Cr^{3+} ion with another. It is possible to get a significant amount of information about these interactions by measuring the paramagnetic resonance spectra of isolated Cr^{3+} single ions and isloated Cr^{3+}-Cr^{3+} pairs of

* Based upon a Ph.D. thesis by R. W. Bené, Stanford University, 1968; supported principally by the National Science Foundation under Grant No GK-1646. Partial support was also supplied by the Joint Services Electronics Program (U. S. Army, U. S. Navy, and U. S. Air Force) under contract No. ONR225(83). The crystals were supplied by the Advanced Research Projects Agency through the Center for Materials Research at Stanford University.

† Present address: Department of Electrical Engineering and Electronics Research Center, The University of Texas, Austin, Tex.

[1] J. F. Dillon, Jr., H. Kamimura, and J. P. Remeika, J. Phys. Chem. Solids **27**, 1531 (1966).

[2] B. Morosin and A. Narath, J. Chem. Phys. **40**, 1958 (1964).

[3] J. F. Dillon, Jr., and J. P. Remeika in *Magnetic and Electric Resonance and Relaxation* edited by J. Smidt (Wiley-Interscience, Inc., New York, 1963), p. 480.

[4] J. F. Dillon, Jr., J. Appl. Phys. Suppl. **33**, 1191 (1962).

[5] J. F. Dillon, Jr., and C. E. Olson, J. Appl. Phys. **36**, 1259 (1965).

ions, which can be created by doping a suitable host material with a small amount of chromium. A suitable host material is one which satisfies three requirements: (1) It must be isostructural to the chromium trihalides, (2) it must be a diamagnetic material, and (3) it must be capable of being doped with chromium.

BiI_3, SbI_3, and AsI_3 are also of space group $R\bar{3}$, and, being diamagnetic, are possible hosts for studying the single-ion pair spectra of a few percent chromium substituted in place of the diamagnetic metal ions. It turns out to be quite possible to dope chromium into BiI_3 and possible to a somewhat lesser extent to dope chromium into SbI_3.

Crystals were grown at Stanford's Center for Materials Research in the central crystal growth laboratory under the direction of R. Fiegelson.

SbI_3 and BiI_3 were grown from the melt by the Bridgman method in quartz crucibles sealed under vacuum. Reagent grade SbI_3 had to be purified by multiple sublimations to a purity of 99.999%. Bismuth iodine was synthesized from elemental bismuth (99.9999%) and I_2 (99.999%) by passing I_2 vapor (in an argon carrier gas) over the Bi sample at 220°C. The product resulting from this synthesis was sublimed several times to remove unreacted bismuth.

The furnace used for crystal growth was a multizone wire-wound resistance type with a cylindrical core. For BiI_3 growth, a steep gradient of 30°C/cm was used, and with SbI_3 about 25°C/cm. Boules were 3 cm long by 1.25 cm in diam. Both SbI_3 and BiI_3 exhibited good cleavage. In the case of SbI_3 easy basal plane cleavage caused single crystals to delaminate easily like mica. The c axis in SbI_3 was perpendicular to the growth axis.

No attempt was made to grow AsI_3.

II. EXPERIMENTAL RESULTS: PARAMAGNETIC RESONANCE SPECTRA OF Cr DOPED INTO BiI_3 AND SbI_3

A. General

The EPR spectra of single crystals of BiI_3 and SbI_3 doped with chromium have been measured at 24 and 35 GHz in magnetic fields up to 18 kOe. Measurements were taken over a temperature range 1.5–77°K, but the bulk of the data was taken at 4.2°K. The spectrometers were standard EPR spectrometers employing magnetic-field modulation and phase-sensitive detection. A recording was made of the first derivative of the absorption. Concentrations of chromium in various crystals, as determined by spectroscopic analysis, were as follows: In $Cr_xBi_{1-x}I_3$, x is varied from 0 to 0.2. In $Cr_xSb_{1-x}I_3$, x is varied from 0 to 0.001. The maximum x value for $Cr_xSb_{1-x}I_3$ represents the maximum amount of chromium that the crystal-growing lab was able to get into SbI_3 using the same techniques that were used for BiI_3: Cr.

B. BiI_3: Cr

The spectrum of chromium doped into BiI_3 consists of a fairly complex assortment of lines. The spectrum is decoded as follows: There is a five-line Cr^{3+} single-ion spectrum, a nine-line Cr^{2+} single-ion spectrum, and a four-line Cr^{3+} pair spectrum. The five-line spectrum for a single Cr^{3+} ion in the BiI_3 host can be fitted by a spin Hamiltonian of the form

$$H_s = g\beta \mathbf{H}\cdot\mathbf{S} + DS_z^2,$$

where $g=2.058\pm0.01$ and $D=0.5\pm0.02$ kOe. Figure 1 shows the energy-level diagram for H along the c axis (H_z) and the pertinent transitions. The three solid arrows are the allowed transitions and the dashed ones are not allowed for this direction of H field but are observed at other angles. The $+\frac{3}{2}\rightarrow-\frac{3}{2}$ transition is not observed, presumably due to the small D value. The $+\frac{3}{2}\rightarrow-\frac{1}{2}$ and $+\frac{1}{2}\rightarrow-\frac{3}{2}$ transitions are also weak due to the small D value, but are observed easily at the high Cr^{3+} concentrations. Their observation is made easier by overloading the microwave cavity with a large sample and thus deforming the rf magnetic field inside to give a component parallel to H_0, the static field. The linewidth of the $+\frac{1}{2}\rightarrow-\frac{1}{2}$ transition is about 135 Oe at low chromium concentration and 4.2°K. The other Cr^{3+} single-ion transitions have linewidths of about 175 Oe. The linewidths increase with chromium concentration and become badly distorted at 10% concentrations, where the linewidth is about 300 Oe. Other small lines appear among the single-ion lines at moderate to large concentrations (1.5% and up), but because the single-ion lines are so large and close together, it is impossible to sort out this additional absorption spectrum. These extra lines, the distortion of the line shape, and the extra linewidth are absent at temperatures as high as 77°K. It is presumed that these lines are due to exchange-coupled pairs with small anisotropy, such as the interlayer pairs.

The nine-line Cr^{2+} single-ion spectrum is the sum of three three-line spectra of Cr^{2+} ions in three different environments. These environments are connected by threefold rotations about the c axis. Each three-line

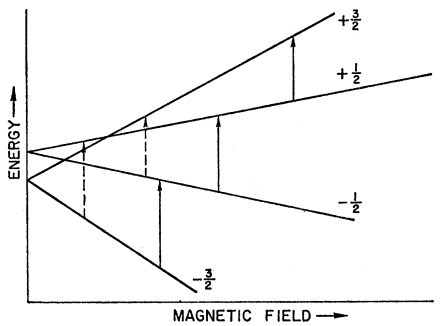

FIG. 1. Energy levels of $H_s=g\beta\mathbf{H}\cdot\mathbf{S}+DS_z^2$ for $H=H_z$.

spectrum can be fitted by a spin Hamiltonian

$$H_s = g\beta \mathbf{H}\cdot\mathbf{S} + DS_z^2 + E(S_x^2 - S_y^2),$$

with $g = 1.98 \pm 0.02$, $D + 6.9 \pm 0.1$ kOe, and $E = 1.6 \pm 0.1$ kOe and $S = 2$. The z axis is about 20° from the c axis and the x axis is the projection of the a axis on the plane perpendicular to the z axis. The D and E are ambiguous within a sign; i.e., they are either both positive or both negative.

The assumption that this spectrum is due to Cr^{2+} is inferred from the following considerations:

(a) The spectrum is fitted by an $S = 2$ spin Hamiltonian.

(b) For a fixed chromium concentration in BiI_3, the intensity of both the Cr^{3+} single-ion transitions and the Cr^{3+}-Cr^{3+} pair transitions are correspondingly low when the intensity for the Cr^{2+} transitions is high.

(c) No other impurities are found by spectroscopic means in some of the crystals, and when they are found they have no correlation with the intensity of the Cr^{2+} lines.

(d) Crystals grown under higher iodine pressure (favoring Cr^{3+} over Cr^{2+}) do not show the nine-line spectrum.

The linewidth of the Cr^{2+} lines is about 125 Oe. The linewidth is somewhat uncertain due to overlapping of the spectra from the three environments. The observed transitions are shown in Fig. 2.

A remark concerning this Cr^{2+} spectrum is in order here. This spectrum represented an undesired complication in the earlier samples used in this experiment. An attempt to fit the spectrum to an $S = \frac{3}{2}$ spin Hamiltonian failed specifically for the low field transition $(+1 \rightarrow -2)$. It was thought that the g value required to fit the frequency variation of this transition [$g = 2.35$ for a $(+\frac{1}{2})$-to-$(-\frac{3}{2})$ transition within $S = \frac{3}{2}$] was unrealistic. Even assuming this g value, the remaining transitions could not be fitted into the $S = \frac{3}{2}$ manifold. As indicated by the rather large error limits of the spin Hamiltonian parameters and the absence of an upper limit on the S^4 term, we have not established the Cr^{2+} spin-Hamiltonian parameters to the same extent as for the Cr^{3+}. The fact that this Cr^{2+} spectrum is incidental to the interactions in the chromium trihalides as well as the experimental difficulties in aligning the external magnetic field along the Cr^{2+} principal axis and in following the small Cr^{2+} transitions underneath the generally much larger Cr^{3+} transitions are the main contributors to this situation. Nevertheless, a large amount of data over all angles of the applied field was consistent with the spin-Hamiltonian parameters given above. The value of $|D|$ is smaller than one might expect for a Cr^{2+} spectrum. We do not know the reason for this.

The four-line Cr^{3+}-Cr^{3+} pair spectrum is fitted by a

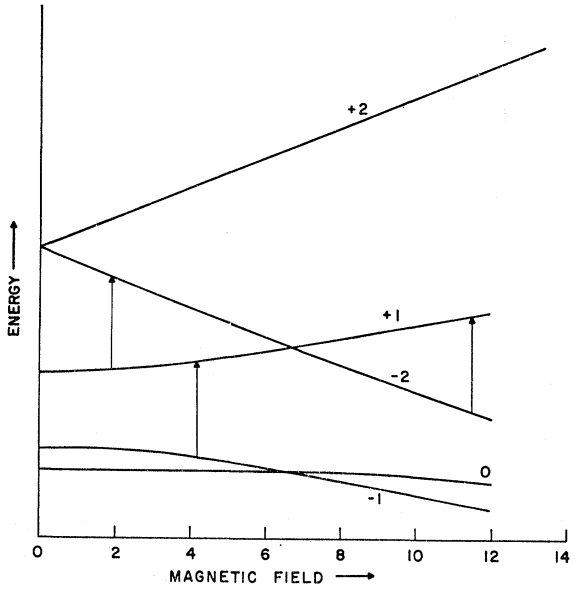

FIG. 2. Energy levels of $H_s = g\beta\mathbf{H}\cdot\mathbf{S} + DS_z^2 + E(S_x^2 - S_y^2)$ for $S = 2$ and $H = H_z$.

spin Hamiltonian of the form

$$H_s = g\beta\mathbf{H}\cdot\mathbf{S} + D(S_{\zeta 1}^2 + S_{\zeta 2}^2) + J(\mathbf{S}_1\cdot\mathbf{S}_2) + \tfrac{3}{2}J_z S_{1z}S_{2z} + \tfrac{1}{4}K(S_1^+S_2^+ + S_1^-S_2^-),$$

where $g = 2.058 \pm 0.02$ and $D = -0.5 \pm 0.25$ kOe are the same as the Cr^{3+} single-ion parameters (except that there is a larger uncertainty in values because of the more complex interaction). $J_z = +34 \pm 2$ kOe, $K = 2.0 \pm 0.25$ kOe, and J is negative (ferromagnetic). The ζ axis is the c axis of the crystal. The negative value for J is consistent with the $S = 3$ manifold being the only one populated at low temperatures, and with the known ferromagnetic intralayer exchange on the order of 14 cm^{-1} for chromium tri-iodide. J_z can be unambiguously assigned a positive value from the temperature dependence of the spectrum, and since K must have the same sign as J to fit the positions of the lines, both are unambiguous. The dipolar interaction has been neglected since the ions are about 4.5 Å apart; thus the dipolar field is about 100 Oe and is smaller than the linewidth of the transitions and is within the error brackets of the other parameters. The four-line Cr^{3+}-Cr^{3+} pair spectrum is really a six-line spectrum, two transitions from each of three separately situated pairs. The lower field transition from each of these pairs (the three pair-bond axis are related by a three-fold rotation about the c axis) is observed only over a very restricted range of angles of the external static magnetic field. Thus in the course of an experiment in which the magnetic field is rotated in a plane, the lower field transition of only *one* of the three differently situated pairs is observed at any given angle. The high field transitions are seen at all angles so that in the course of an experiment we observe

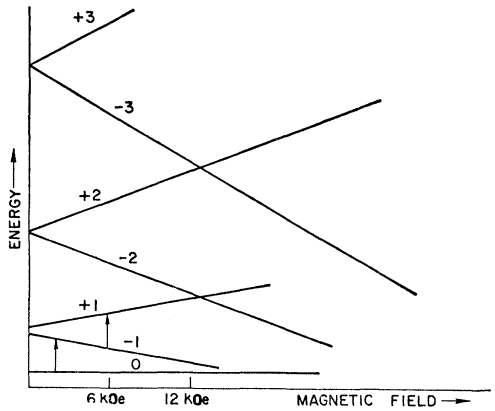

FIG. 3. Energy levels of pair Hamiltonian for $S=3$ and H along z axis of pairs.

four transitions due to the pairs. Figure 3 shows a plot of the energy levels for the $S=3$ manifold for the two coupled $S=\frac{3}{2}$ Cr^{3+} ions. The external field is along the z axis of the pairs (perpendicular to the plane containing the Cr^{3+}-Cr^{3+} pair and the two halogens through which the dominant superexchange interaction takes place). The two transitions which are seen are indicated in Fig. 3.

The linewidth for the -1 to 1 transition is about 110 Oe. The narrowest linewidth for the 0 to 1 transition is about the same, but the absorption broadens very rapidly as the external field moves away from true alignment with the z axis, since the 0 and -1 energy levels become almost parallel in this region of magnetic field.

The ratio of the intensity of the pair lines to the single-ion lines follows approximately a c (concentration) dependence for chromium concentrations less than about 5%. The exceptions are the crystals for which Cr^{2+} lines have large intensity; for these crystals the pair to single-ion intensity ratio is less than would be expected from the concentration given by spectroscopic analysis for total chromium content.

The background noise in the spectrum of BiI_3:Cr is a conglomeration of small, fairly broad (70 Oe or more) lines. It is possible that these absorptions are due to triads and interlayer pairs under the single-ion lines, since they seem to increase in relative intensity with the concentration of chromium.

C. SbI_3: Cr

The spectrum of SbI_3:Cr is a fairly straightforward six-line spectrum arising from single Cr^{3+} ions. In this case the D value is large enough that the $\frac{3}{2}\rightarrow-\frac{3}{2}$ transition is easily seen. The spin Hamiltonian is given by

$$H_s=g_{||}\beta H_z S_z+g_\perp\beta(H_xS_x+H_yS_y)+DS_z^2,$$

with $g_{||}=2.078\pm0.01$, $g_\perp=2.088\pm0.01$, and $D=+3.85\pm0.05$ kOe. The z axis is the threefold c axis of the structure. The maximum concentration attainable is 0.1%, so that Cr^{3+}-Cr^{3+} pairs are not seen. A Cr^{2+} single-ion spectrum is not seen in this material.

III. THEORETICAL INTERPRETATION OF EXPERIMENTAL RESULTS

A. g Value

Two of the most surprising features of the experimental results are the g value and the large anisotropy of the exchange interaction.

Simple ionic crystal field theory leads one to the conclusion that the g value for an ion with a *less* than half-filled shell should be slightly less than the free spin value (2.0023). For the present case of the Cr^{3+} ion, the configuration is d^3, so that we might expect a g value of less than 2, as is indeed usually observed in the oxides. The presently observed values are 2.058 in BiI_3, and 2.07 in SbI_3. The key to the discrepancy lies in the large spin-orbit constant on the halogens and the fact that these materials are quite covalent.

In the present case we take the unit structure as a Cr^{3+} ion surrounded by six halogen (H^-) ions in an octahedral coordination. Figure 4 shows this unit structure, the coordinate system, and the numbering of the halogens. There is a reasonably large overlap between the Cr^{3+} single electron $3d$ orbitals and the halogen p orbitals, so that we must take combinations of the d orbitals and the halogen p orbitals as the basic one-electron orbitals. Convenient forms for these, which have the correct site symmetry, are the molecular orbitals.

An example of such an orbital which transforms as the xy component of the t_{2g} representation of cubic symmetry, is shown in Fig. 5, where the center orbit is a d_{xy} orbit of Cr^{3+} at A, and the others are halogen p_x or p_y orbitals centered at positions 1, 2, 4, and 5.

There are actually two orbitals that might be represented by the above picture, the antibonding $t_{2g}{}^a(xy)$ orbital and the bonding $t_{2g}{}^b(xy)$ orbital.

$$t_{2g}{}^a(xy)=\gamma d_{xy}{}^A-\tfrac{1}{2}(1-\gamma^2)^{1/2}[p_{y_1}-p_{y_4}+p_{x_2}-p_{x_5}],$$
$$t_{2g}{}^b(xy)=\tfrac{1}{2}\gamma[p_{y_1}-p_{y_4}+p_{x_2}-p_{x_5}]+(1-\gamma^2)^{1/2}d_{xy}{}^A.$$

The γ is close to 1, and both the above cases describe π bonds, since the p orbits are perpendicular to the bond axis. Clearly the antibonding orbital is mainly of $d_{xy}{}^A$

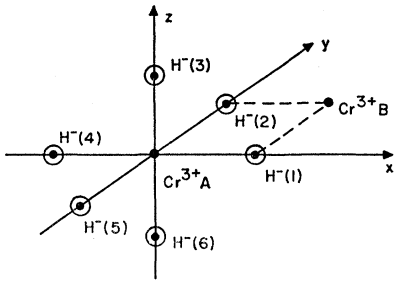

FIG. 4. Coordination of $[Cr^{3+}H^-{}_6]^{3-}$ complex.

character and the bonding orbital is mainly of halogen character. Because the ionic d energy levels are higher than the ionic halogen p levels, the d-like (antibonding) state will be higher in energy than the halogenlike (bonding) state. To emphasize the physical differences in the states, we make the following notation change:

$$t_{2g}{}^{a} \longrightarrow t_{2g},$$
$$t_{1g}{}^{n} \longrightarrow t_{1g}{}^{p},$$
$$t_{2g}{}^{b} \longrightarrow t_{2g}{}^{p}.$$

We make the obvious change for all other states also. The p indicates the p-like halogen character of the bonding and nonbonding orbitals, and the antibonding orbitals correspond closely to the ionic d-like orbitals. Figure 6 shows the energy levels of the molecular orbitals for the $[Cr^{3+}H^{-}{}_{6}]^{3-}$ complex.

The squares represent the number of *occupied* states in the ionic approximation in the regions just to the left and right of the molecular orbital region in the center of Fig. 6. The squares on the extreme left side represent the *occupied* states of the chromium atom. The circles in the molecular orbital region in the center represent the *possible* orbital states in the molecular orbital approximation. Each state can, of course, have spin up or down. The occupations shown by the arrows indicating spin up and spin down represent the $|{}^4A_{2g}\rangle$ ground state of the complex which is in the configuration $(t_{2g})^3$. We shall adopt the usual convention of dropping the filled shells from the designation of the configuration, because they will make no contribution to the results in the calculations that we consider.

For the orbitally singlet ground state, like $|{}^4A_{2g}\rangle$, the g value to first order is given by the spin-only value

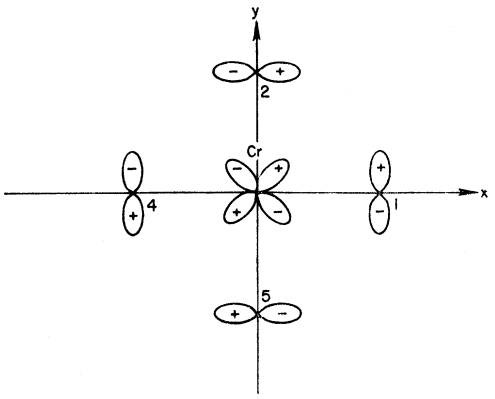

FIG. 5. A $t_{2g}(XY)$ molecular orbital.

2.0023. The spin-orbit energy will, however, mix excited states into the ground state (destroying its ${}^4A_{2g}$ designation). In particular, since L and S both transform like T_{1g}, spin orbit will mix $|{}^2T_{2g}\rangle$ and $|{}^4T_{2g}\rangle$ states into the $|{}^4A_{2g}\rangle$ ground state. There will then be a second-order contribution to the g value proportional to

$$\sum_n \frac{\langle {}^4A_{2g}|H_{so}|n\rangle\langle n|\mathbf{H}\cdot\mathbf{L}|{}^4A_{2g}\rangle}{E_0-E_n},$$

where $|n\rangle$ is an excited state.

Since the orbital Zeeman term $\mathbf{H}\cdot\mathbf{L}$ does not involve spin, $|n\rangle$ must be a spin quartet if $\langle n|\mathbf{H}\cdot\mathbf{L}|{}^4A_{2g}\rangle$ is not to vanish, and therefore the only form of $|n\rangle$ which enters the calculation for g is a $|{}^4T_{2g}\rangle$ state. There are various $|{}^4T_{2g}\rangle$ excited states which are obtained by the excitation of an electron from a low-lying state to an e_g state. The three most important excitations are shown by the

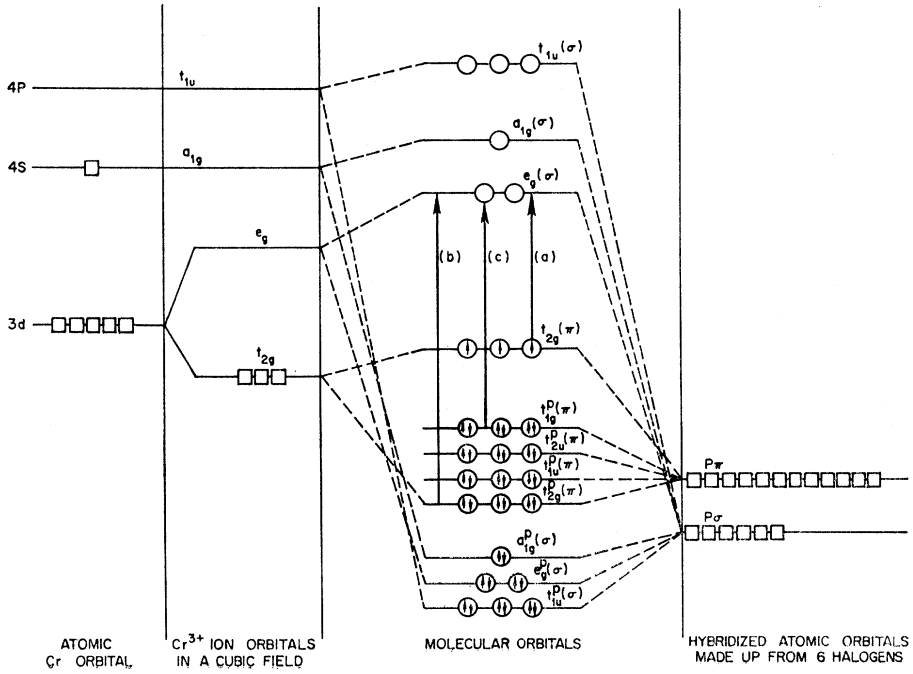

FIG. 6. Molecular orbitals for the $[Cr^{3+}H^{-}{}_{6}]^{3-}$ complex.

arrows in Fig. 6. Configuration (a) is a d-like configuration $(t_{2g}{}^a)^2 e_g{}^a$ since the antibonding orbitals are d-like. In the absence of covalent bonding, this would correspond to the $(t_{2g})^2 e_g$ configuration. This state is obtained by promoting one of the Cr^{3+} d electrons from a t_{2g} level to the higher energy Cr^{3+} e_g level. The g shift, due to coupling to the state $|(t_{2g})^2 e_g\, {}^4T_{2g}\rangle$, is that usually computed for Cr^{3+} and is negative. (See Appendix A for numerical estimates.) The effect of the covalent bonding on the contribution from this state is to reduce the magnitude of the g shift. This is generally represented by an orbital reduction factor.

There are two possible $|{}^4T_{2g}\rangle$ states for configuration (b), which is indicated by $(t_{2g})^3 e_g (t_{2g}{}^p)^5$. The $|e_g\, {}^2E_g\rangle$ state can be coupled to the $|(t_{2g})^3\, {}^4A_{2g}\rangle$ state to give either a $|{}^5E_g\rangle$ state or a $|{}^3E_g\rangle$ state, and either can couple to the $|(t_{2g}{}^p)^5\, {}^2T_{2g}\rangle$ state to give a final $|{}^4T_{2g}\rangle$ state for configuration (b). Likewise there are two $|{}^4T_{2g}\rangle$ states for configuration (c), $(t_{2g})^3 e_g (t_{1g}{}^p)^5$. The configuration $(t_{2g})^3 e_g (t_{2g}{}^p)^5$ represents an excited configuration for which there has been a transfer from a predominantly halogen orbital (t_{2g} bonding) to a d-like orbital (e_g antibonding). Thus configuration (b) represents a "charge-transfer" configuration.

A list of the configurations and $|{}^4T_{2g}\rangle$ states which are important for a calculation of the g value, are the following:

Configuration	States
(a) $(t_{2g})^2 e_g$	$\|(t_{2g})^2 e_g\, {}^4T_{2g}\rangle$
(b) $(t_{2g})^3 e_g (t_{2g}{}^p)^5$	$\|(t_{2g})^3\, {}^4A_{2g} e_g\, {}^2E_g({}^5E_g)(t_{2g}{}^p)^5\, {}^2T_{2g}({}^4T_{2g})\rangle$
and	$\|(t_{2g})^3\, {}^4A_{2g} e_g\, {}^2E_g({}^3E_g)(t_{2g}{}^p)^5\, {}^2T_{2g}({}^4T_{2g})\rangle$
(c) $(t_{2g})^3 e_g (t_{1g}{}^p)^5$	$\|t(_{2g})^3\, {}^4A_{2g} e_g\, {}^2E_g({}^5E_g)(t_{1g}{}^p)^5\, {}^2T_{1g}({}^4T_{2g})\rangle$
and	$\|(t_{2g})^3\, {}^4A_{2g} e_g\, {}^2E_g({}^3E_g)(t_{1g}{}^p)^5\, {}^2T_{1g}({}^4T_{2g})\rangle$.

Here, for instance, $|(t_{2g})^3\, {}^4A_{2g} e_g({}^5E_g)(t_{2g}{}^p)^5\, {}^2T_{2g}({}^4T_{2g})\rangle$ means the state where the configuration $(t_{2g})^3$ in the state $|{}^4A_{2g}\rangle$ is coupled to configuration e_g in the state $|{}^2E_g\rangle$ to form a state $|{}^5E_g\rangle$. This state is then coupled to the configuration $(t_{2g}{}^p)^5$ in the state $|{}^2T_{2g}\rangle$ to form the final $|{}^4T_{2g}\rangle$ state.

In the ionic limit the matrix element $\langle {}^4A_{2g}|H_{so}|{}^4T_{2g}\rangle$ vanishes for $|{}^4T_{2g}\rangle$ states of configuration (b) and (c). This is because we take H_{so} as a single-electron operator and $\langle (t_{2g})^3 (t_{2g}{}^p)^6|H_{so}|(t_{2g})^3 e_g (t_{2g}{}^p)^5\rangle$ vanishes if e_g and $t_{2g}{}^p$ are spatially separated from one another. In the above matrix element, H_{so} represents a sum over nine electrons, but can be broken up into a sum over three electrons and six electrons.

$$\begin{aligned}\langle (t_{2g})^3 (t_{2g}{}^p)^6|H_{so}|(t_{2g})^3 e_g (t_{2g}{}^p)^5\rangle &= \langle (t_{2g})^3|H_{so}|(t_{2g})^3\rangle\langle (t_{2g}{}^p)^6|(t_{2g}{}^p)^5 e_g\rangle \\ &\quad + \langle (t_{2g}{}^p)^6|H_{so}|(t_{2g}{}^p)^5 e_g\rangle\langle (t_{2g})^3|(t_{2g})^3\rangle \\ &= \langle (t_{2g}{}^p)^6|H_{so}|(t_{2g}{}^p)^5 e_g\rangle .\end{aligned}$$

In Appendix A we show that the second matrix element is proportional to $\langle t_{2g}{}^p|H_{so}|e_g\rangle$ and will be zero unless there is some region of overlap between the $t_{2g}{}^p$ and e_g orbitals.

In the presence of covalent bonding the states of configurations (b) and (c) do make a contribution to the g shift. These transfer configurations are all of the form d^4p^5, and since the spin-orbit constant on the halogens is up to 30 times that of the Cr^{3+} ions, the p part dominates. We have, therefore, a predominantly one-hole situation which gives a negative effective spin-orbit parameter and a positive g shift. As shown in Appendix A, the magnitudes of these shifts for each of the configurations (b) and (c) are the same order of magnitude as the negative shift from configuration (a). For CrI_3 the shift from (a) is on the order of -0.02, from (b) $+0.025$ and from (c) $+0.02$. Thus we would predict a net positive g shift, which is what we observe experimentally. Quite a few numerical estimates of atomic and molecular parameters must be made in computing the value of the positive shift in g value, so that only the sign and the order of magnitude of the g shift are probably meaningful. We calculate in detail the contribution to the g shift from only the most important $|{}^4T_{2g}\rangle$ states, because an exhaustive calculation for all possible $|{}^4T_{2g}\rangle$ states will not change the sign or order of magnitude of the g shift. The only other states for which the energy denominator of Eq. (A7) is approximately the same as for the configurations (a)–(c) (calculated explicitly) are configurations of the form $(t_{2g})^4 (t_{2g}{}^p)^5$ and $(t_{2g})^4 (t_{1g}{}^p)^5$. The contribution from these configurations is expected to be small, however, because the fourth d electron is π bonded. (The e_g orbital was σ bonded.) As shown in Appendix A, the g shift is proportional to the square of the bond strength, and so the contribution from a configuration where the fourth electron is π bonded will be an order of magnitude smaller than the contribution from a configuration where the fourth electron is σ bonded.

B. Exchange Anisotropy

We have determined experimentally that the exchange anisotropy between two intralayer Cr^{3+} ions is approximately 3 cm^{-1}, and is almost axial. The principal axis of the exchange anisotropy is the perpendicular to the plane containing the pair of Cr^{3+} ions and the two halogens through which the dominant superexchange interaction takes place. This axis is the z axis of Appendix B and is shown in Fig. 7.

If we assume that the isotropic exchange integral is about the same (within a factor of 1.5) for a pair of Cr^{3+} ions in BiI_3 as it is for CrI_3, then the ratio of the anisotropic exchange constant to the isotropic exchange constant is about $-\frac{1}{5}$. (The interlayer isotropic exchange constant for CrI_3 is approximately 14 cm^{-1} and ferromagnetic, which means $J_{iso} \cong -14$ cm^{-1}.) The assumption concerning the near equality of the exchange integrals in BiI_3 and CrI_3 is reasonable since the lattice constants in BiI_3 are only 6–10% larger than those in

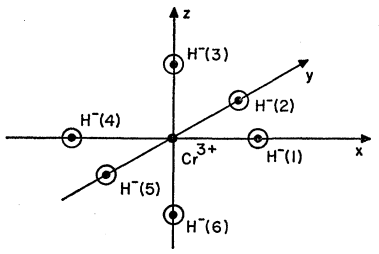

FIG. 7. The coordinate axis for the intralayer $Cr^{3+}-Cr^{3+}$ pair, and the numbering of the H^- (halogen) ions making up the octahedral environment of the Cr^{3+} A ion.

CrI_3. This assumed small difference in exchange constants can be compared to the difference in isotropic exchange constants in CrI_3 and $CrCl_3$, where there is a further decrease in the lattice parameters of 15–20% in addition to the change in identity of the ligand through which the superexchange takes place; the J_{iso} in CrI_3 is still only $\frac{5}{2}$ times that in $CrCl_3$.

The models to date have predicted[6] that $|J_{aniso}/J_{iso}| \approx (\Delta g/g)^2$. This is clearly not the case for Cr pairs in BiI_3 because $(\Delta g/g)^2 \cong 0.001$, and $|J_{aniso}/J_{iso}| \approx \frac{1}{5}$. The reason for this discrepancy, as for the positive shift of the g value, has its roots in the large covalency and the large spin-orbit constant of the ligands. As seen in the g-value calculation, the covalency and halogen spin-orbit interaction mix into the $|^4A_{2g}\rangle$ ground state a significant amount of $|^4T_{2g}\rangle$ and $|^2T_{2g}\rangle$ transfer states. These states make an important contribution to the exchange interaction between ions because they have an appreciable amount of ligand character. Thus, the transfer states have much more overlap with the ground-state wavefunction of a neighboring Cr ion, than the ground state of the first Cr ion would have. That is, ${}_B\langle {}^4A_{2g}|H_{ex}{}^{AB}|{}^4T_{2g}\rangle_A \gg {}_B\langle {}^4A_{2g}|H_{ex}{}^{AB}|{}^4A_{2g}\rangle_A$ because $|{}^4T_{2g}\rangle_A$ is spatially closer to $|{}^4A_{2g}\rangle_B$ than $|{}^4A_{2g}\rangle_A$ is.

The interaction via the transfer states is highly anisotropic because the exchange interaction between the $|{}^4A_{2g}\rangle_B$ state on ion B and the XY component of the $|{}^4T_{2g}\rangle_A$ state of ion A is generally different from the interaction between the $|{}^4A_{2g}\rangle_B$ state and the XZ or YZ components of the $|{}^4T_{2g}\rangle_A$ state. This difference in the interactions is reasonable on physical grounds since the two Cr^{3+} ions and the two halogens through which the interaction must take place lie in the X-Y plane. We might expect the states transforming as XZ and YZ would have little effect on the interaction between the two Cr^{3+} ions. The spin components are coupled to the components of the $|{}^4T_{2g}\rangle$ state differently because of the isotropic $(\zeta'\mathbf{L}\cdot\mathbf{S})$ spin-orbit interaction: i.e., the S_z component of spin couples to the XY component of the $|{}^4T_{2g}\rangle$ state which is admixed into the $|{}^4A_{2g}\rangle$ ground state by L_z. Thus the difference in the exchange interaction between the $|{}^4A_{2g}\rangle_B$ state and the different components of the $|{}^4T_{2g}\rangle_A$ state produces an anisotropic spin interaction. The spin Hamiltonian is derived in more detail in Appendix B.

This spin Hamiltonian is very complex, so that we have calculated the difference in energy between $|3,3\rangle$ state and the $|3,0\rangle$ state as a measure of the anisotropy. These are states of the two coupled Cr^{3+} ions with total spin$=3$ and the z components given by $M_s=3$ or 0. The z axis is the same as the z axis of Fig. 6 and is *not* the c axis.

We stress here that in the absence of spin-orbit interaction on the halogens (or if it were significantly smaller, as in the oxides) the transfer states would not be appreciably admixed into the ground state, and the usual estimates of the anisotropy $\cong(\Delta g/g)^2\ J_{iso}$ would be essentially correct.

The isotropic part of the exchange interaction is given predominantly by ${}_B\langle {}^4A_{2g}|H_{ex}{}^{AB}|{}^4A_{2g}\rangle_A$. This matrix element really stands for the sum of exchange integrals over all pairs of orbits, one orbit on ion A and the other on ion B. The orbits we use are the three molecular orbitals which are occupied in the $|{}^4A_{2g}\rangle$ ground state. By using molecular orbitals we have implicitly included the kinetic transfer contribution to the exchange as far out as the ligands. If we should then set the exchange Hamiltonian equal to the Coulomb potential between molecular orbitals, we would be including everything except the direct Cr-Cr transfer part of the kinetic exchange. The exchange integrals designated as $J_{p\text{-}d}$ or $J_{p\text{-}p}$ turn out to be dominant in these materials. These integrals do not involve Cr-Cr transfer and therefore are calculated as matrix elements of the Coulomb interaction between molecular orbitals. The kinetic transfer is already taken into account for the p-p and p-d interactions by the bonding coefficients of the molecular orbitals which appear in front of the $J_{p\text{-}p}$ and $J_{p\text{-}d}$ integrals in the calculations. For the smaller $J_{d^A d^B}$ exchange integrals we have not specified the specific form of the exchange interaction, but have left the results in a form which allows us to include the direct Cr-Cr kinetic transfer in the interpretation of the particular exchange integral. (That is, we include both Coulombic and kinetic energy in the exchange Hamiltonian and evaluate matrix elements between molecular orbitals.) For example, to represent the exchange between a dxy orbital on A and a dxy orbital on B we have written $J_{dxy\,{}^A dxy^B}$. There are three important contributions to $J_{dxy\,{}^A dxy^B}$. (1) There a is direct Coulomb interaction between the dxy orbitals. This interaction is expected to be quite small since the Cr^{3+} ions are about $\frac{9}{2}$ Å apart. (2) The direct transfer interaction between a dxy orbital on A and a dxy orbital on B takes place because of the kinetic-energy term in the exchange Hamiltonian. This interaction is antiferromagnetic and is probably fairly small due to the large distance between ions. (3) There is also a direct kinetic transfer between a dxy orbital on A and a d_{z^2} or $d_{x^2-y^2}$ orbital on B. This effect is ferromagnetic and the transfer integral is probably larger than for the type-(2) transfer due to

[6] T. Moriya, Phys. Rev. **120**, 91 (1960).

the "easy" path through the ligands. However, this interaction is intrinsically smaller than the type-(2) interaction by a factor of $J_{\text{Hunds}}/U_{\text{ion}}$. ($J_{\text{Hund}}$ is the Hund's-rule energy of a Cr^{2+} ion, and U_{ion} is the ionization energy required to change a Cr^{3+} ion to a Cr^{2+} ion). Thus, contributions (2) and (3) tend to cancel and are probably about the same order of magnitude.

In the calculation we assume that the exchange interaction between all of the individual pairs of orbits is isotropic. This is a good approximation for the $J_{p\text{-}p}$ (Hund's rule interaction on a halogen ion) and the kinetic transfer parts of the $J_{d^A d^B}$ interaction. The anisotropy in the aforementioned type-(2) transfer has been worked out in detail, taking into account the anisotropy of the d^4-d^2 excited state by which the transfer interaction takes place. The complexity and length of the calculation together with the result that contribution to anisotropy is negligible for small $(\Delta g)^2/g^2$, makes it undersirable to reproduce this calculation here. It is not true that the J_{p-d} of $J_{d^A d^B}$ (Coulombic part) exchanges are completely isotropic, but again the anisotropy is small for a small $(\Delta g)^2/g^2$ ratio.

The results of the calculation estimate that $J_{\text{aniso}}/J_{\text{iso}} \simeq -0.16$ for CrI_3.

C. Summary of Theoretical Results

In summary, we would stress that when there is appreciable covalency in the problem, the single-ion parameters are really a characteristic of a complex such as $[Cr^{3+}H^-_6]^{3-}$ (where H^- designates a halogen) and not just those of Cr^{3+} in an octahedral environment; or even Cr^{3+} in an octahedral environment with X amount of covalent bonding. The actual identity of the halogen is important through the magnitude of its spin-orbit parameter. We must also consider the total $[Cr^{3+}H^-_6]^{3-}$ complex when calculating the exchange interaction between two ions when the superexchange via the ligands is the dominant part of the isotropic exchange.

IV. EXPLANATION OF g VALUE AND MAGNETIC ANISOTROPY IN CHROMIUM TRIHALIDES

A. g Value

We now extend the interpretation of the measurements on BiI_3:Cr and SbI_3:Cr to the magnetic series $CrCl_3$, $CrBr_3$, and CrI_3. The variation of the g value in this series is qualitatively what we would expect on the basis of the calculation in Appendix A. Due to the large variation in the halogen spin-orbit constants and also the moderate variation in the bonding parameters, we would expect the positive g shift caused by the transfer states to be about $\frac{1}{3}$ in the $CrBr_3$ of that in CrI_3 and in $CrCl_3$ to be about $\frac{1}{10}$ of that in CrI_3. We would also expect the negative g shift to vary much more slowly going from $CrCl_3$ to $CrBr_3$ to CrI_3 because of the slow variation of $10Dq$. Thus we might expect the g values of the series to be something like the following:

$$\begin{aligned} CrCl_3 &\quad 1.99, \\ CrBr_3 &\quad 2.01, \\ CrI_3 &\quad 2.07, \end{aligned}$$

where we have assumed that the negative g shift is about -0.02 (Appendix A), and that the positive g shift is enough to account for the g value of CrI_3. These are not in bad agreement with the reported values;

$$\begin{aligned} CrCl_3 &\quad 2.00, \\ CrBr_3 &\quad 2.007, \\ CrI_3 &\quad 2.07, \end{aligned}$$

but the small difference in the measured values between $CrCl_3$ and $CrBr_3$ is slightly perplexing in view of the difference between the g values of CrI_3 and $CrBr_3$. For some reason, either the positive shift of the g value in $CrCl_3$ is larger than we expect or the negative shift is smaller.

B. Macroscopic Magnetic Anisotropy

The interpretation of the magnetic anisotropy in the chromium trihalides is more complex than the interpretation of the g value because there are three distinct physical parameters which determine the total magnetic anisotropy. These are (1) The anisotropy energy constant of a single ion and the diamagnetic lattice; (2) the exchange constant which describes the anisotropic part of the exchange energy between an intralayer pair of Cr^{3+} ions; and (3) the angle which the axis of anisotropy of exchange makes with the c axis of the crystal.

We really have only two experimental facts upon which to base an approximation of the single-ion anisotropy in the chromium trihalides: The D values in BiI_3:Cr and SbI_3:Cr. In BiI_3:Cr the value of D is -0.05 cm^{-1}, and in SbI_3:Cr it is $+0.38$ cm^{-1}. The single-ion anisotropy depends on the trigonal distortion of the structure. This distortion is roughly proportional to the deviation from 54.7° of the angle between the c axis and a line between the Cr^{3+} ion and any one of its nearest-neighbor halogens. [Note that (a) all three such lines make the same angle with the c axis, and (b) this is the same angle which the c axis makes with the previously defined z axis, which is the third parameter.] The D value becomes more negative as this angle is increased. If we calculate the angles for BiI_3 and SbI_3 as well as the chromium trihalide series we find that they decrease in the following order [2,7,8]:

$$BiI_3,\ SbI_3,\ CrI_3,\ CrBr_3,\ CrCl_3.$$

[7] H. Braekken, Kgl. Norske Videnskab. Selskabs, Forh. **5**, 42 (1932).

[8] R. W. G. Wyckoff, *Crystal Structures* (Wiley-Interscience, Inc., New York, 1964), Vol. 2, p. 45.

Thus on purely structural grounds we expect the D value to go more positive going from BiI_3 to $CrCl_3$. If only the nearest halogens to the Cr^{3+} ion were important the D value for all of the above series should be negative, because all angles appear to be greater than 54.7°. The next-nearest halogens in layers above and below the nearest halogens undoubtedly enter into the distortion, however. The angles of the nearest of these are somewhat less than 40° and so would be expected to make a positive contribution. The positive contribution to the distortion from the next-nearest neighbors could easily be the same order of magnitude as the negative contribution from the nearest neighbors due to the small deviation from 54.7° of the angle previously calculated. In $CrCl_3$ this angle was calculated to be $5.55°\pm1°$, and in BiI_3 it was calculated to be 57.5°. We also expect the spin-orbit interaction on the halogens to significantly affect the single-ion anisotropy since it is argued that this interaction produces the major part of the g shift. Since the single-ion anisotropy is proportional to the square of the spin-orbit constant times the σ bond strength, we expect a great reduction in the positive single-ion anisotropy constant going from CrI_3 to $CrBr_3$ to $CrCl_3$.

Thus based on these arguments and the values for D in BiI_3 and SbI_3 measured in our experiments, we predict roughly the following single-ion constants:

$$\begin{aligned} BiI_3 &\quad -0.05\ \text{cm}^{-1}, \\ SbI_3 &\quad +0.38\ \text{cm}^{-1}, \\ CrI_3 &\quad +0.38\ \text{cm}^{-1}, \\ CrBr_3 &\quad +0.08\ \text{cm}^{-1}, \\ CrCl_3 &\quad 0. \end{aligned}$$

In arriving at the value of D in CrI_3 we used the fact that the c/a ratio for SbI_3 is about that of CrI_3, and we assumed the same σ bonding strength. We conclude from these rather crude approximations that the single-ion anisotropy is an order of magnitude too small and has the wrong sign to account for the experimental macroscopic magnetic anisotropy in the chromium trihalides.

We thus turn to the anisotropy of the exchange interaction to account for the macroscopic observations. As calculated in Appendix B, we expect the ratio of the anisotropic exchange to the isotropic exchange to vary as the square of the halogen spin-orbit constant times the strength of the σ bond. We therefore expect this ratio to go as 1:0.2:0.01 in the series CrI_3, $CrBr_3$, and $CrCl_3$. If the constant describing the pair-exchange anisotropy is approximately the same in CrI_3 as it is in BiI_3, we would expect the following values for that constant (J_z') for the chromium trihalide family:

$$\begin{aligned} &CrI_3\ J_z' = 5\ \text{cm}^{-1}, \\ &CrBr_3\ J_z' = 1\ \text{cm}^{-1}, \\ &CrCl_3\ J_z' = 0.05\ \text{cm}^{-1}. \end{aligned}$$

The angle that we have called the third parameter determines how much of this single-pair-anisotropy of exchange is translated into a macroscopic magnetic anisotropy such as one measures in a static torque measurement or in a ferromagnetic resonance measurement. The contribution of the uniaxial anisotropy of exchange to the ferromagnetic resonance frequency can be shown to be $S\sum Z_p J_p'(3\cos^2\theta - 1)$.[9] The sum over p is a sum over all the different types of pairs, Z_p is the number of neighbors which form a given type of pair p with the central ion, and J_p' is the axial anisotropic exchange constant for that type of pair. θ is the angle the exchange anisotropy axis of a pair makes with the c axis. When $\theta = 54.7°$, the total macroscopic anisotropy is zero, even for arbitrarily large pair anisotropy. In BiI_3 this angle is measured to be $57.5°\pm2°$. If we take the atom positions given by x-ray analysis,[2,7] we calculate this angle to be $55.5°\pm1.0°$ for $CrCl_3$ and 56.6° for $CrBr_3$. The atom positions have not been measured to our knowledge for CrI_3. However, the c/a ratios for the chromium trihalides are very close to the same value. They are

$$(c/a)_{CrCl_3} = 2.92, \quad (c/a)_{CrBr_3} = 2.907, \quad (c/a)_{CrI_3} = 2.898.$$

In view of this small variation in the c/a ratio, one might expect that the variation in the angle that the c axis makes with the plane of the Cr-Cr pairs would only be of the order of 0.5° from one trihalide to another. The ratios are such that CrI_3 has the largest angle. Unfortunately, these angles are close enough to the critical 54.7° that the uncertainty in the lattice positions results in a large uncertainty in the total anisotropy.

If we use our estimate of the exchange anisotropy constants and assume angles of 57°, 56.5°, and 56° for CrI_3, $CrBr_3$, and $CrCl_3$, respectively, then we can use the aforementioned equation to calculate the contribution of anisotropic exchange to the anisotropy constant which shifts the magnitude of the applied static magnetic field required for ferromagnetic resonance. (Again, this is the same anisotropy that one would measure in a static torque experiment.) Table I compares the experimental anisotropy constants with those calculated. Column 1 lists the exchange anisotropy contribution to total anisotropy. Column 2 lists the

TABLE I. Comparison of exchange anisotropy to observed total anisotropy in the chromium trihalides

	Predicted macroscopic anisotropy arising from exchange anisotropy	Estimated single-ion anisotropy $2DS$	Total estimated anisotropy	Observed macroscopic anisotropy (excluding dipolar terms)
	(cm^{-1})	(cm^{-1})	(cm^{-1})	(cm^{-1})
CrI_3	−2.4	1.14	−1.26	−2.75
$CrBr_3$	−0.36	+0.24	−0.12	−0.66
$CrCl_3$	≃0	≃0	≃0	−0.19

[9] J. Kanamori, in *Magnetism*, edited by G. Rado and H. Suhl (Academic Press Inc., New York, 1963), Vol. 1, p. 127.

single-ion anisotropy previously roughly estimated from the structures and the measured values for BiI_3 and SbI_3. Column 3 is a sum of columns 1 and 2, and column 4 is the observed macroscopic anisotropy. It is clear from columns 1 and 4 that the exchange anisotropy is of the correct order of magnitude and sign to account for the total magnetic anisotropy. Apparently, the single-ion anisotropy is of the opposite sign than the measured total anisotropy.

ACKNOWLEDGMENTS

I wish to thank Professor R. L. White for many stimulating and helpful conversations held during the course of this work, and for his critical reading of this manuscript. I wish also to thank R. Feigelson and H. Swartz for growing the crystals used in this study.

APPENDIX A: g VALUE

The ground state of a Cr^{3+} ion in an octahedral environment is the orbital singlet $^4A_{2g}$. Thus the g value, to first order, is the spin-only value 2.0023. When the spin-orbit interaction energy is considered as a perturbation the first-order ground state becomes

$$\frac{1}{N}\{|^4A_{2g}\rangle+\sum_i \delta_i|^4T_{2g}\rangle+\sum_i n_i|^2T_{2g}\rangle\}, \quad \text{(A1)}$$

where the i are summed over all states which can be described in the cubic field as $|^4T_{2g}\rangle$ or $|^2T_{2g}\rangle$ states. Only the $|^4T_{2g}\rangle$ states will contribute in second order to the g value since the orbital Zeeman term $\mathbf{H}\cdot\mathbf{L}$ has nonzero matrix elements only between $|^4T_{2g}\rangle$ and $|^4A_{2g}\rangle$ states.

The $|^4T_{2g}\rangle$ states come from various configurations. We will discuss the five $|^4T_{2g}\rangle$ states which have the dominant effect on the g value; these come from the following configurations:

(a) d-like $(t_{2g})^2e_g$ (one state),

(b) $(t_{2g})^3e_g(t_{2g}{}^p)^5$ (two states),

(c) $(t_{2g})^3e_g(t_{1g}{}^p)^5$ (two states).

The t_{2g} and e_g are the cubic field symmetry labels for the antibonding single particle molecular orbitals, and the $t_{2g}{}^p$ and $t_{1g}{}^p$ represent bonding orbitals made up mostly of halogen p orbitals.

The state in configuration (a) is the one usually treated by standard perturbation theory; it gives a negative contribution to the g value. We estimate that

$$\Delta g=-8K\zeta_d/3U\approx-0.02 \text{ for } Cr^{3+} \text{ in } CrI_3. \quad \text{(A2)}$$

The effect of covalent bonding is accounted for by inclusion of the orbital reduction factor K. Configuration (b) has two $|^4T_{2g}\rangle$ states which we designate by

$$\begin{aligned}&|(t_{2g})^3\,{}^4A_{2g}e_g\,{}^2E_g({}^5E_g)(t_{2g}{}^p)^5\,{}^2T_{2g}({}^4T_{2g})\rangle,\\&|(t_{2g})^3\,{}^4A_{2g}e_g\,{}^2E_g({}^3E_g)(t_{2g}{}^p)^5\,{}^2T_{2g}({}^4T_{2g})\rangle;\end{aligned} \quad \text{(i)}$$

$$\begin{aligned}&|(t_{2g})^3\,{}^4A_{2g},e_g\,{}^2E_g(t_{2g}{}^p)^5\,{}^2T_{2g}({}^3T_{1g})({}^4T_{2g})\rangle,\\&|(t_{2g})^3\,{}^4A_{2g},e_g\,{}^2E_g(t_{2g}{}^p)^5\,{}^2T_{2g}({}^1T_{1g})({}^4T_{2g})\rangle.\end{aligned} \quad \text{(ii)}$$

In the first set of states (i) we couple the $|e_g\rangle$ state to the $|(t_{2g})^3\,{}^4A_{2g}\rangle$ state first and then couple to the $|(t_{2g}{}^p)^5\,{}^2T_{2g}\rangle$ state. In states (ii) we couple the $|e_g\rangle$ state to the $|(t_{2g})^3\,{}^4A_{2g}\rangle$ state. Since the Coulombic interaction on the Cr^{3+} ion is much larger than the exchange between the Cr^{3+} ion and a halogen, the states in set (i) are probably close to the eigenstates of the system and thus are the states used in the perturbation calculation. However, in order to do the calculation it is necessary to expand the approximate eigenstates (i) in terms of states (ii). The expansion can be made using the appropriate Racah parameters as follows:[10]

$$\begin{aligned}&\phi(j_1,(j_2j_3)j_{23},JM)\\&\quad=\sum_{j_{12}}\phi((j_1j_2)j_{12},j_3,JM)[(2j_{12}+1)(2j_{23}+1)]^{1/2}\\&\qquad\times W(j_1j_2Jj_3;\,j_{12}j_{23}).\end{aligned} \quad \text{(A3)}$$

The Racah W parameters are given in terms of the 6-j symbols as follows:

$$\begin{Bmatrix}j_1 & j_2 & j_3\\ l_1 & l_2 & l_3\end{Bmatrix}=(-1)^{j_1+j_2+l_1+l_2}W(j_1j_2l_2l_1;\,j_3l_3). \quad \text{(A4)}$$

The 6-j symbols have been tabulated by Rotenberg *et al.*[11] Finally we obtain

$$\begin{aligned}&|({}^5E_g)\,{}^4T_{2g}\rangle\\&\quad=\tfrac{1}{4}\sqrt{2}\{(\sqrt{5})|({}^1T_{1g})\,{}^4T_{2g}\rangle+\sqrt{3}|({}^3T_{1g})\,{}^4T_{2g}\rangle\},\\&|({}^3E_g)\,{}^4T_{2g}\rangle\\&\quad=\tfrac{1}{4}\sqrt{2}\{-\sqrt{3}|({}^1T_{1g})\,{}^4T_{2g}\rangle+(\sqrt{5})|({}^3T_{1g})\,{}^4T_{2g}\rangle\}.\end{aligned} \quad \text{(A5)}$$

Using the appropriate Clebsh-Gordan (CG) coefficients,[12] we can expand the nine-electron $|^4T_{2g},\gamma,M_s\rangle$ and $|^4A_{2g},M_s\rangle$ states in terms of products of the antisymmetrized three-electron $|(t_{2g})^3\,{}^4A_{2g}M_s\rangle$ states with the six-electron $|(t_{2g}{}^p)^5\,{}^2T_{2g}e_g\,{}^2E_g\,{}^3T_{1g},\gamma,M_s\rangle$ and $|(t_{2g}{}^p)^5\,{}^2T_{2g}e_g\,{}^2E_g\,{}^1T_{1g},\gamma,0\rangle$ states. We obtain

$$|^4A_{2g},M_s\rangle=|(t_{2g})^3\,{}^4A_{2g},M_s\rangle|(t_{2g}{}^p)^6\,{}^1A_{1g},0\rangle,$$

$$\left|({}^1T_{1g})\,{}^4T_{2g},\begin{pmatrix}\xi\\ \eta\\ \zeta\end{pmatrix},M_s\right\rangle=|(t_{2g})^3\,{}^4A_{2g},M_s\rangle\left|(t_{2g}{}^p)^5e_g\,{}^1T_{1g},\begin{pmatrix}\alpha\\ \beta\\ \gamma\end{pmatrix},0\right\rangle,$$

[10] A. R. Edmonds, *Angular Momentum in Quantum Mechanics* (Princeton University Press, Princeton, New Jersey, 1957), p. 90.
[11] M. Rotenberg, R. Bivins, N. Metropolis, and J. K. Wooten, Jr., *The 3-j and 6-j Symbols* (Technology Press, M. I. T., Cambridge, Mass., 1959).
[12] E. U. Condon and G. H. Shortley, *The Theory of Atomic Spectra* (Cambridge University Press, New York, 1967), Sec. 1–8.

and

$$\left|(^3T_{1g})\,^4T_{2g},\begin{pmatrix}\xi\\ \eta\\ \zeta\end{pmatrix},M_s\right\rangle=\left(\frac{(\frac{3}{2}-M_s)(\frac{3}{2}+M_s+1)}{\frac{15}{2}}\right)^{1/2}\left|(t_{2g})^3\,^4A_{2g},M_s+1\right\rangle\left|(t_{2g}{}^p)^5e_g\,^3T_{1g},\begin{pmatrix}\alpha\\ \beta\\ \gamma\end{pmatrix},-1\right\rangle$$
$$+\frac{M_s}{(15/4)^{1/2}}\left|(t_{2g})^3\,^4A_{2g},M_s\right\rangle\left|(t_{2g}{}^p)^5e_g\,^3T_{1g},\begin{pmatrix}\alpha\\ \beta\\ \gamma\end{pmatrix},0\right\rangle-\left(\frac{(\frac{3}{2}+M_s)(\frac{3}{2}-M_s+1)}{\frac{15}{2}}\right)^{1/2}\left|(t_{2g})^3\,^4A_{2g},M_s-1\right\rangle \quad \text{(A6)}$$
$$\times\left|(t_{2g}{}^p)^5e_g\,^3T_{1g},\begin{pmatrix}\alpha\\ \beta\\ \gamma\end{pmatrix},+1\right\rangle.$$

We have written the orbital components in order within the parentheses on both sides of each equation so that we need not write each equation for the $|T_{2g}\rangle$ states three times.

Matrix elements of spin-orbit and orbital angular momentum between $|^4A_{2g}\rangle$ states and $|^4T_{2g}\rangle$ states can be written down for H_{so} and H_{oz} as a sum over the nine single-particle operators. (H_{oz} is the orbital Zeeman interaction $g\beta\mathbf{H}\cdot\mathbf{L}$.) As shown in Ref. 12, the $|(t_{2g})^3\,^4A_{2g}\rangle$ part will factor out of the problem and we will be left with H_{so} and H_{oz} for the six remaining electrons.

After the factorization we find that the second-order contribution to the g value from configuration (b) is

$$\Delta g_z=-4\sum_{\gamma,i}\frac{\langle{}^4A_{2g},\tfrac{1}{2}|L_z|{}^4T_{2g},\gamma,\tfrac{1}{2}\rangle_{ii}\langle{}^4T_{2g},\gamma,\tfrac{1}{2}|H_{so}|{}^4A_{2g},\tfrac{1}{2}\rangle}{U_i}, \quad \text{(A7)}$$

where γ specifies the orbital component of the $|^4T_{2g}\rangle$ state and $i=1$, 2 indicates which $|^4T_{2g}\rangle$ state of this configuration is involved. The factor of 4 outside the summation comes from two sources: one factor of 2 arises because we are combining a term plus its complex conjugate, and the second factor of 2 arises because we are evaluating the matrix elements for the $m_s=\frac{1}{2}$ states.

Remembering now that the above $|^4T_{2g}\rangle$ states are the $|(^5E_g)\,^4T_{2g}\rangle$ and $|(^3E_g)\,^4T_{2g}\rangle$ states, expanding these in terms of the $|(^3T_{1g})\,^4T_{2g}\rangle$ and $|(^1T_{1g})\,^4T_{2g}\rangle$ states and, in turn, these in terms of the product states, we get

$$\Delta g_z=-4\left(\frac{1}{U(^5E_g)}-\frac{1}{U(^3E_g)}\right)\frac{\sqrt{15}}{8}\frac{1}{\sqrt{15}}$$
$$\times\sum_\gamma\langle(t_{2g}{}^p)^6\,^1A_1,0|L_z|(t_{2g}{}^p)^5e_g\,^1T_{1g},\gamma,0\rangle$$
$$\times\langle(t_{2g}{}^p)^5e_g\,^3T_{1g},\gamma,0|H_{so}|(t_{2g}{}^p)^6\,^1A_1,0\rangle. \quad \text{(A8)}$$

We can evaluate the above matrix elements using the tensor-operator methods of Tanabe and Kamimura (TK).[13] Using their formulas (2.3) and (2.13), and assuming an isotropic spin-orbit interaction operator (i.e., $\sum_i\zeta_i\mathbf{l}_i\cdot\mathbf{s}_i$) we get the Δg_z in terms of the reduced matrix elements.

$$\Delta g_z=+4\left(\frac{1}{U(^5E)}-\frac{1}{U(^3E)}\right)\frac{1}{24\sqrt{3}}$$
$$\times((t_{2g}{}^p)^6\,^1A_1\|T_1\|(t_{2g}{}^p)^5e_g\,^1T_{1g})$$
$$\times((t_{2g}{}^p)^5e_g\,^3T_{1g}\|V(^1T_1)\|(t_{2g}{}^p)^6\,^1A_1). \quad \text{(A9)}$$

[13] Y. Tanabe and H. Kamimura, J. Phys. Soc. Japan **13**, 394 (1958).

Using Eqs. (2.6) and (2.9) of TK we get

$$(^1A_1\|T_1\|{}^1T_1)=-(-1)(^1T_1\|T_1\|{}^1A_1)=+(^1T_1\|T_1\|{}^1A_1).$$

If we use the footnote on p. 403 of TK, in which electrons are effectively replaced by their equivalent holes, and then use Eqs. (2.35)–(2.39), we get

$$(^1T_1\|T_1\|{}^1A_1)=-\sqrt{2}(t_2\|t\|e)$$

and

$$(^3T_1\|T_1\|{}^1A_1)=-2\sqrt{6}(\tfrac{1}{2}t_2\|st\|\tfrac{1}{2}e)(-1/2\sqrt{6})$$
$$=+(\tfrac{1}{2}t_2\|st\|\tfrac{1}{2}e). \quad \text{(A10)}$$

The first minus sign on the second line and the resultant plus sign are the result of the hole character of the $(t_{2g}{}^p)^5\,^2T_{2g}$ configuration. We obtain

$$\Delta g_z=-\frac{1}{3\sqrt{6}}\left(\frac{1}{U(^5E)}-\frac{1}{U(^3E)}\right)(t_2\|t\|e)(\tfrac{1}{2}t_2\|st\|\tfrac{1}{2}e)$$
$$=-\left(\frac{1}{U(^5E)}-\frac{1}{U(^3E)}\right)\langle t_{2g}{}^p,\zeta|t_1,\gamma|e_g,V\rangle$$
$$\times\langle\tfrac{1}{2}t_{2g}{}^p,\tfrac{1}{2},\zeta|\zeta' l_z s_z|\tfrac{1}{2}e_g,\tfrac{1}{2},V\rangle \quad \text{(A11)}$$

using the CG coefficients.[14]

The matrix elements in the second line of (A11) are evaluated using molecular orbitals where, for example, the spin-orbit contribution is approximately the sum of $\zeta'\mathbf{l}_i\cdot\mathbf{S}_i$ for the various parts of the molecular orbital. The molecular orbital is made up of a Cr d-like part and a halogenlike part. When operating on a molecular orbital with the spin-orbit operator $\mathbf{l}_i\cdot\mathbf{S}_i$, we operate on the different parts separately. We assume that $\mathbf{l}_i$ is

[14] Y. Tanabe and S. Sugano, J. Phys. Soc. Japan **9**, 753 (1954).

the orbital angular momentum operator with respect to the chromium nucleus for the d-like part and $\mathbf{l}_i$ is taken as the orbital angular momentum operator with respect to a halogen nucleus when operating on a halogen part of the molecular orbital. That this is the correct method is clear from the derivation in Slichter[15] for the g value of a V_k center. The matrix elements of l_z are measured the same way. This is in contrast to the usual method where H_{so} or l_z operating on a molecular orbital is taken as the operator with respect to the center of the entire orbital reduced by an "orbital reduction factor." The $|t_{2g}{}^p,\zeta\rangle$ state is the XY component of the t_{2g} bonding orbitals and can be written as

$$|t_{2g}{}^p,\zeta\rangle=|XY\rangle^b$$
$$=\tfrac{1}{2}\beta[P_{y_1}-P_{y_4}+P_{x_2}-P_{x_5}]+(1-\beta^2)^{1/2}dxy. \quad \text{(A12)}$$

Likewise,

$$|e_g,V\rangle=|X^2-Y^2\rangle^a$$
$$=\alpha d_{x^2-y^2}-\tfrac{1}{2}(1-\alpha^2)^{1/2}[P_{x_4}-P_{x_1}+P_{y_2}-P_{y_5}],$$

where, for example P_{y_1} is the P_y orbital at ligand 1. The numbers of the ligands and the coordinate system are shown in Fig. 4. The x, y, and z directions are the same for all ligands. Using (A12) to evaluate the matrix elements in (A11) we get

$$\langle XY|L_z|X^2-Y^2\rangle=i[2\alpha(1-\beta^2)^{1/2}+\beta(1-\alpha^2)^{1/2}],$$
$$\langle\tfrac{1}{2},XY|\zeta' L_zS_z|\tfrac{1}{2},X^2-Y^2\rangle \quad \text{(A13)}$$
$$=\tfrac{1}{2}[2\alpha(1-\beta^2)^{1/2}\zeta_d+\beta(1-\alpha^2)^{1/2}\zeta_I].$$

Therefore,

$$\Delta g_z=+\tfrac{1}{2}[1/U(^5E)-1/U(^3E)]$$
$$\times[2\alpha(1-\beta^2)^{1/2}+\beta(1-\alpha^2)^{1/2}]$$
$$\times[2\alpha(1-\beta^2)^{1/2}\zeta_d+\beta(1-\alpha^2)^{1/2}\zeta_I]. \quad \text{(A14)}$$

Everything from (A9)–(A14) has been independent of the orbital and spin components of the original $|{}^4T_{2g}\rangle$ state. If we calculate Δg_x and Δg_y by taking the proper matrix elements to calculate ΔE to second order, we find that $\Delta g_x=\Delta g_y=\Delta g_z=\Delta g$ as must be the case for cubic coordination.

We estimate the approximate value of Δg. $U(^5E)$ is the energy required to transfer an electron from a $t_{2g}{}^p$ bonding orbital to an e_g antibonding orbital. From the work of Dillon *et al.*[1] we estimate this at about 25 000 cm^{-1}. Also $U(^3E)-U(^5E)\cong 6B+5C$ and is approximately 20 000 cm^{-1} for CrI_3. The spin-orbit constants for the chromium ion and the Cl, Br, and I atoms are approximately[1]

$$\zeta_{3d}\cong 290 \text{ cm}^{-1},$$
$$\zeta_{Cl}\cong 590 \text{ cm}^{-1},$$
$$\zeta_{Br}\cong 2460 \text{ cm}^{-1},$$
$$\zeta_{I}\cong 5070 \text{ cm}^{-1}.$$

[15] C. P. Slichter, *Principles of Magnetic Resonance* (Harper and Row, New York, 1963), p. 195.

The parameter α^2 is associated with a σ bond and was estimated for $CrCl_3$ and $CrBr_3$ by Barnes and Segal[16] using experimental nuclear quadrupole resonance frequencies. They obtained

$$\alpha^2(CrCl_3)\cong 0.76,$$
$$\alpha^2(CrBr_3)\cong 0.73.$$

Thus for the more covalent CrI_3 we will estimate $\alpha^2\cong 0.70$ or $1-\alpha^2\cong 0.3$. The β^2 describes a π bond which is probably slightly less than an order of magnitude weaker than the σ bond. We take $1-\beta^2\cong 0.04$.

Using these numbers we get

$$\Delta g_I\cong+0.025,$$
$$\Delta g_{Br}\cong+0.01,$$
$$\Delta g_{Cl}\cong+0.002.$$

We now repeat all of the preceding calculations for the two $|{}^4T_{2g}\rangle$ states of configuration (c). The calculation is very similar to the one that we just did for configuration (b) and so we will not write down all of the steps. We do need to rederive Eqs. (2.34)–(2.39) in TK for matrix elements involving t_{1g} orbitals instead of t_{2g} orbitals, but this rederivation turns out to be a trivial replacement of f_2 (or t_{2g}) by f_1 (or t_{1g}) in the equations. The one new constant that we get is not tabulated but is easily calculated. The two new molecular orbitals we need to use for configuration (c) are antibonding:

$$|Z^2\rangle^a=\alpha d_{z^2}-\tfrac{1}{6}\sqrt{3}(1-\alpha^2)^{1/2}$$
$$\times[2P_{z_6}-2P_{z_3}+P_{x_1}-P_{x_4}+P_{y_2}-P_{y_5}],$$

nonbonding:

$$|Z\rangle^n=\tfrac{1}{2}[P_{y_1}-P_{y_4}+P_{x_5}-P_{x_2}].$$

After we carry out the same steps as before we get

$$\Delta g=+\tfrac{1}{6}\sqrt{3}(1-\alpha^2)\zeta_I[1/U(^5E)-1/U(^3E)],$$

where α^2 again represents a σ bond, but the $U(^5E)$ this time represents the energy required to transfer an electron from the t_{1g} nonbonding orbital to the e_g antibonding orbital. We estimate[1] this energy as $\cong$15 000 cm^{-1}. We get

$$\Delta g_I\cong+0.02,$$
$$\Delta g_{Br}\cong+0.008,$$
$$\Delta g_{Cl}\cong+0.002.$$

APPENDIX B: EXCHANGE ANISOTROPY

The symmetric part of anisotropic exchange enters in third-order perturbation theory. A second-order term which consists of a matrix element of spin-orbit energy times a matrix element of exchange gives a contribution to antisymmetric exchange. This term vanishes in the present case, however, where all Cr^{3+} sites are equivalent. For the terms which are diagonal in the exchange inter-

[16] R. G. Barnes and S. L. Segal, Phys. Rev. Letters 3, 462 (1959).

action the anisotropy energy ΔE has the following form:

$$\Delta E=\sum_n \frac{\langle g|H_{so}|n\rangle\langle n|H_{ex}|n\rangle\langle n|H_{so}|g\rangle}{(E_n-E_g)^2}, \quad \text{(B1)}$$

where $|g\rangle$ is the ground state of two-ion problem (i.e., both ion A and ion B are in $|{}^4A_{2g}\rangle$ states) and $|n\rangle$ is an excited state for the two-ion problem, which is connected to $|g\rangle$ via H_{so}. This restricts $|n\rangle$ to be a state with one ion in the $|{}^4A_{2g}\rangle$ ground state and the other in a $|{}^4T_{2g}\rangle$ state or a $|{}^2T_{2g}\rangle$ state.

Because ions A and B are equivalent, we can write (B1) as

$$\Delta E=2\sum_n \frac{\langle g|H_{so}{}^B|n\rangle\langle n|H_{ex}|n\rangle\langle n|H_{so}{}^B|g\rangle}{(E_n-E_g)^2},$$

where we have separated the spin-orbit operator into two parts, $H_{so}=H_{so}{}^A+H_{so}{}^B$, which give equal contributions to ΔE. Since $|g\rangle$ and $|n\rangle$ are basis states for a spin-independent Hamiltonian, we can treat spin as a parameter and derive the spin Hamiltonian.[17] Accordingly, assuming an isotropic spin-orbit interaction, we can write

$$\langle g|H_{so}{}^B|n\rangle=\lambda\sum_{i=x,y,z} S_i\langle g|L_i{}^B|n\rangle. \quad \text{(B2)}$$

For states $|n\rangle$ representing two-ion states with ion A in a $|{}^4A_{2g}\rangle$ state and ion B in a $|{}^4T_{2g}\rangle$ state we can write

$$\begin{aligned}\langle g|L_i{}^B|n\rangle&={}_B\langle {}^4A_{2g},e_g|L_i|\ {}^4T_{2g},\gamma\rangle_B\\&=({}^4A_{2g}\|T_1\|{}^4T_{2g})(A_2e_2|T_2\gamma T_1\gamma_i),\end{aligned} \quad \text{(B3)}$$

where we have expanded the matrix element as a product of a reduced matrix element and a CG coefficient. For each γ_i there is only one γ for which the CG coefficient is nonzero. [That is, for $\gamma_i=Z$, $(A_2e_2|T_2\ XY\ T_1Z)=-\frac{1}{3}\sqrt{3}$ and all other CG coefficients involving $\gamma_i=Z$, but $\gamma\neq XY$ are 0.] Substituting (B3) into (B2) and evaluating the CG coefficients we find

$$\begin{aligned}\langle g|H_{so}{}^B|n\rangle=&-(\lambda/\sqrt{3})({}^4A_{2g}\|T_{1g}\|{}^4T_{2g})\\&\times\{S_x(n\xi)+S_y(n\eta)+S_z(n\zeta)\},\end{aligned} \quad \text{(B4)}$$

where, e.g., $S_x(n\xi)$ indicates S_x connects $|g\rangle$ to the state $|n\rangle$ which is made up of ion A in the $|{}^4A_{2g}\rangle$ state and ion B in the ξ component of the $|{}^4T_{2g}\rangle$ state. We introduce here the notation $\xi=YZ$, $\eta=XZ$, and $\zeta=XY$. Thus,

$$\begin{aligned}\Delta E=\sum_n \frac{2\lambda^2}{3}\frac{|\langle {}^4A_{2g}\|T_{2g}\|{}^4T_{2g}\rangle|^2}{(E_n-E_g)_2}&\langle S_x(n\xi)+S_y(n\eta)\\&+S_z(n\zeta)|H_{ex}|S_x(n\xi)+S_y(n\eta)+S_z(n\zeta)\rangle.\end{aligned} \quad \text{(B5)}$$

We now consider a particular $|n\rangle$ which represents a two-ion state in which ion A is in a $|{}^4A_{2g}\rangle$ state and ion B is in a $|{}^5(E_g)\ {}^4T_{2g}\rangle$ state of configuration (b). (See Appendix A for specification of the configurations.) We assume that the exchange interaction between two components of the ionic states is approximately isotropic; i.e., for the exchange interaction between ions we set

$$\langle n,\xi|H_{ex}{}^{AB}|n,\xi\rangle=J_{AB}{}^{\xi\xi}\mathbf{S}^A\cdot\mathbf{S}^B. \quad \text{(B6)}$$

Although we are assuming that the exchange interaction between any two components of the ionic states is *isotropic*, we are not assuming that the exchange interaction between two component states is *equal* to the interaction between another two component states, e.g.,

$$\langle n,\xi|H_{ex}{}^{AB}|n\langle\xi\rangle\neq\langle n,\zeta|H_{ex}{}^{AB}|n,\zeta\rangle$$

or

$$J_{AB}{}^{\xi\xi}\neq J_{AB}{}^{\zeta\zeta}.$$

If we substitute for all of the matrix elements in (B5) terms similar to the one given by (B6), we obtain the following spin Hamiltonian:

$$\Delta E=H_s=\frac{2\lambda^2}{3}\frac{|\langle {}^4A_{2g}\|T_{2g}\|{}^4T_{2g}\rangle|^2}{[U({}^5E_g)]^2}\left\{\begin{array}{l}S_x{}^B(\mathbf{S}^A\cdot\mathbf{S}^B)S_x{}^BJ_{AB}{}^{\xi\xi}+S_y{}^B(\mathbf{S}^A\cdot\mathbf{S}^B)S_y{}^BJ_{AB}{}^{\eta\eta}\\+S_z{}^B(\mathbf{S}^A\cdot\mathbf{S}^B)S_z{}^BJ_{AB}{}^{\zeta\zeta}\\+[S_x{}^B(\mathbf{S}^A\cdot\mathbf{S}^B)S_y{}^B+S_y{}^B(\mathbf{S}^A\cdot\mathbf{S}^B)S_x{}^B]J_{AB}{}^{\xi\eta}\\+[S_x{}^B(\mathbf{S}^A\cdot\mathbf{S}^B)S_z{}^B+S_z{}^B(\mathbf{S}^A\cdot\mathbf{S}^B)S_x{}^B]J_{AB}{}^{\xi\zeta}\\+[S_y{}^B(\mathbf{S}^A\cdot\mathbf{S}_z{}^B+S_z{}^B(\mathbf{S}^A\cdot\mathbf{S}^B)S_y{}^B]J_{AB}{}^{\eta\zeta}\end{array}\right\}. \quad \text{(B7)}$$

If the spin were $\frac{1}{2}$, it would be possible to express the above spin Hamiltonian in the usual simplified form, $J_xS_x{}^AS_x{}^B+J_yS_y{}^AS_y{}^B+J_zS_z{}^AS_z{}^B$, but for $S=\frac{3}{2}$ this is not possible. In order to compare the magnitude of the exchange anisotropy predicted by (B7) with experiment we calculate

$$\langle 3,3|H_s|3,3\rangle-\langle 3,0|H_s|3,0\rangle.$$

We first expand each two-ion state in terms of products of single-ion states using the appropriate CG coefficients.

$$\begin{aligned}|3,3\rangle&=|\tfrac{3}{2},\tfrac{3}{2}\rangle_A|\tfrac{3}{2},\tfrac{3}{2}\rangle_B,\\|3,0\rangle&=\frac{1}{\sqrt{20}}\left\{\begin{array}{l}|\tfrac{3}{2},\tfrac{3}{2}\rangle_A|\tfrac{3}{2},-\tfrac{3}{2}\rangle_B+|\tfrac{3}{2},-\tfrac{3}{2}\rangle_A|\tfrac{3}{2},\tfrac{3}{2}\rangle_B\\+3|\tfrac{3}{2},\tfrac{1}{2}\rangle_A|\tfrac{3}{2},-\tfrac{1}{2}\rangle_B+3|\tfrac{3}{2},-\tfrac{1}{2}\rangle_A|\tfrac{3}{2},\tfrac{1}{2}\rangle_B\end{array}\right\}.\end{aligned} \quad \text{(B8)}$$

[17] T. Nagamiya, K. Yosida, and R. Kubo, Advan. Phys. 4, 1 (1955).

Using Eqs. (7) and (8) and a considerable amount of simple algebra we get;

$$\begin{aligned}\langle 3,3|H_s|3,3\rangle &= (9/8)(J_{AB}{}^{\prime\xi\xi}+J_{AB}{}^{\prime\eta\eta}) \\ &\quad +(81/8)J_{AB}{}^{\prime\zeta\zeta}, \\ \langle 3,0|H_s|3,0\rangle &= (261/40)(J_{AB}{}^{\prime\xi\xi}+J_{AB}{}^{\prime\eta\eta}) \\ &\quad -(27/40)J_{AB}{}^{\prime\zeta\zeta},\end{aligned} \tag{B9}$$

where $J_{AB}{}^{\prime\xi\xi}=(\lambda^2|\langle {}^4A_{2g}\|T_{1g}\|{}^4T_{2g}\rangle|^2/3U^2)J_{AB}{}^{\xi\xi}$ and similarly for $J_{AB}{}^{\prime\eta\eta}$ and $J_{AB}{}^{\prime\zeta\zeta}$. If we define $E_{\text{aniso}}=\langle 3,3|H_s|3,3\rangle-\langle 3,0|H_s|3,0\rangle$, then we have

$$E_{\text{aniso}}=(27/5)[2J_{AB}{}^{\prime\zeta\zeta}-J_{AB}{}^{\prime\xi\xi}-J_{AB}{}^{\prime\eta\eta}]. \tag{B10}$$

At this point we should note two things. We are assuming that each ion sees a perfectly cubic octahedral crystalline field which accounts for the coefficients of the terms $J_{AB}{}^{\prime\zeta\zeta}$, $J_{AB}{}^{\prime\xi\xi}$, and $J_{AB}{}^{\prime\eta\eta}$ being in the ratio $2:-1:-1$ in the anisotropy energy. If we should also assume that $J_{AB}{}^{\xi\xi}=J_{AB}{}^{\eta\eta}=J_{AB}{}^{\zeta\zeta}$, as is often done, we would get $E_{\text{aniso}}=0$. The exchange integrals involve two Cr^{3+} ions and thus the symmetry, which the different components of exchange must satisfy, is much less than cubic. In the present case there is no reason for assuming the contributions to exchange between ions from the different components of the excited states should be equal. On the contrary, it seems intuitively clear that the contribution to exchange from the different components of the excited states will *not* be equal because of the different spatial distributions of these components. Secondly, the form of the spin Hamiltonian is independent of which particular $|{}^4T_{2g}\rangle$ state we are considering, so that E_{aniso} (total for all $|{}^4T_{2g}\rangle$ states is simply the sum of contributions, each described by Eq. (B7). We simply calculate the J_{AB}, etc., for each configuration.

We must now approximate the J_{AB} for the various components of particular states. The component eigenstates of configuration (b) consist of products of components of the $|(t_{2g})^3e_gE_g\rangle$ state times the components of the $|(t_{2g}{}^p)^5\,{}^2T_{2g}{}^p\rangle$ state. The particular combination of components of the E_g and ${}^2T_{2g}$ states which are present in the final $|{}^4T_{2g}\rangle$ coupled state is determined by the appropriate CG coefficients. In Eq. (B11) we give those components of a coupled $|{}^4T_{2g}\rangle$ eigenstate in terms of components of the E_g and ${}^2T_{2g}$ states.

$$\begin{aligned}|T_{2g}(\xi)\rangle &= |T_{2g}{}^p(\xi)\rangle[\tfrac{1}{2}\sqrt{3}\,|E_g(V)\rangle-\tfrac{1}{2}|E(U)\rangle], \\ |T_{2g}(\eta)\rangle &= |T_{2g}{}^p(\eta)\rangle[\tfrac{1}{2}\sqrt{3}\,|E_g(V)\rangle+\tfrac{1}{2}|E(U)\rangle], \\ |T_{2g}(\zeta)\rangle &= |T_{2g}{}^p(\zeta)\rangle|E(U)\rangle.\end{aligned} \tag{B11}$$

In these states $U\infty V^2$ and $V\infty X^2-Y^2$. We have dropped the spin notation in Eq. (B11) because it is immaterial to the relations: i.e., the relations in Eq. (B11) are the same whether the E_g state is a ${}^3E_g$ state or a ${}^5E_g$ state. The p in $|T_{2g}{}^p(\gamma)\rangle$ states on the right-hand-side of the equation emphasizes that these states are halogenlike.

The matrix elements of exchange that we require are all diagonal matrix elements and therefore can be calculated as the sum of exchange integrals of all possible pairs of orbits in the state $|n\gamma\rangle(\gamma=\xi,\ \eta,\ \text{or}\ \zeta)$. Since we are only interested in exchange between ions A and B, we must merely sum up all of the exchange integrals between pairs of orbits, one being on each ion. For configuration (b) the orbits to consider are

ion A: $(t_{2g})^3$ (three orbits) $(t_{2g}{}^p)^6$ (six orbits)

ion B: $(t_{2g})^3$ (three orbits) e_g (one orbit)
$(t_{2g}{}^p)^5$ (five orbits).

To be more explicit, we will now approximate $J_{AB}{}^{\xi\xi}$ for the state $|({}^5E)\,{}^4T_{2g}\rangle$. From Appendix A: $|({}^5E)\,{}^4T_{2g}\rangle=\frac{1}{2}(\sqrt{\frac{5}{2}})|({}^1T_1)\,{}^4T_{2g}\rangle+\frac{1}{2}(\sqrt{\frac{3}{2}})|({}^3T_1)\,{}^4T_{2g}\rangle$. Therefore, for this state,

$$\begin{aligned}J_{AB}{}^{\xi\xi}=&\{\text{sum of exchanges of each } t_{2g} \text{ orbital on} \\ &B \text{ with all of those on } A\} \\ &+\{\text{exchange of } e_g(\xi)=[\tfrac{1}{2}\sqrt{3}e(X^2-Y^2) \\ &-\tfrac{1}{2}e(Z^2)] \text{ with all orbits on } A\} \\ &+(\tfrac{3}{8}\text{-}\tfrac{5}{8})\{\text{exchange of unpaired } t_{2g}{}^p(\xi) \text{ orbit} \\ &\text{with all orbits on } A\}.\end{aligned} \tag{B12}$$

We now note two things. The $(t_{2g}{}^p)^6$ closed shell on ion A can be dropped from the calculation as the total exchange with any other orbital will be zero. Secondly, the last two parentheses would change signs if we were calculating the contribution to J_{AB} from the $|({}^3E)\,{}^4T_{2g}\rangle$ state instead of the $|({}^5E)\,{}^4T_{2g}\rangle$ state.

We again use molecular orbitals for the calculation, although we might anticipate some nonorthogonality problems. Figure 8 shows the coordinates and ligand positions used for the calculation.

The orbitals required on ion A are the t_{2g} antibonding orbitals. They are π-bonded.

$$\begin{aligned}|XY\rangle_A{}^a &= \gamma d_{xy}{}^A-\tfrac{1}{2}(1-\gamma^2)^{1/2}[P_{y_1}-P_{y_4}+P_{x_2}-P_{x_5}], \\ |YZ\rangle_A{}^a &= \gamma d_{yz}{}^A-\tfrac{1}{2}(1-\gamma^2)^{1/2} \\ &\quad \times[P_{y_3}-P_{y_6}+P_{x_2}-P_{x_5}], \\ |XZ\rangle_A{}^a &= \gamma d_{xz}{}^A-\tfrac{1}{2}(1-\gamma^2)^{1/2}[P_{x_3}-P_{x_6}+P_{z_1}-P_{z_4}].\end{aligned} \tag{B13}$$

The orbitals required on ion B are the following:

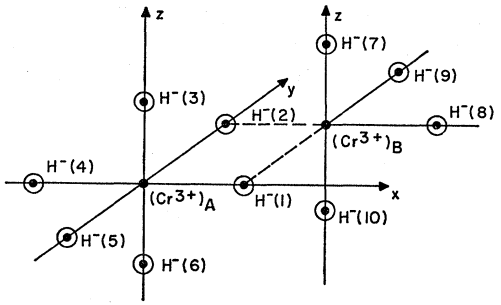

FIG. 8. Coordination of Cr^{3+}-Cr^{3+} pair and their nearest-neighbor halogen.

The antibonding t_{2g} orbitals (π-bonded):

$$|XY\rangle_B{}^a=\gamma d_{xy}{}^B-\tfrac{1}{2}(1-\gamma^2)^{1/2}[P_{y_8}-P_{y_2}+P_{x_9}-P_{x_1}],$$
$$|YZ\rangle_B{}^a=\gamma d_{yz}{}^B-\tfrac{1}{2}(1-\gamma^2)^{1/2}\times[P_{y_7}-P_{y_{10}}+P_{z_9}-P_{z_1}], \quad \text{(B14)}$$
$$|XZ\rangle_B{}^a=\gamma d_{xz}{}^B-\tfrac{1}{2}(1-\gamma^2)^{1/2}[P_{x_7}-P_{x_{10}}+P_{z_8}-P_{z_2}].$$

The bonding $t_{2g}{}^p$ orbitals (π-bonded):

$$|XY\rangle_B{}^b=\tfrac{1}{2}\beta[P_{y_8}-P_{y_2}+P_{x_9}-P_{x_1}]+(1-\beta^2)^{1/2}d_{xy}{}^B,$$
$$|YZ\rangle_B{}^b=\tfrac{1}{2}\beta[P_{y_7}-P_{y_{10}}+P_{z_9}-P_{z_1}]+(1-\beta^2)^{1/2}d_{yz}{}^B,$$
$$|XZ\rangle_B{}^b=\tfrac{1}{2}\beta[P_{x_7}-P_{x_{10}}+P_{z_8}-P_{z_2}]+(1-\beta^2)^{1/2}d_{xz}{}^B.$$

The antibonding e_g orbitals (σ-bonded):

$$|Z^2\rangle_B{}^a=\alpha d_{z^2}{}^B-\tfrac{1}{6}\sqrt{3}(1-\alpha^2)^{1/2}\times[P_{x_8}-P_{x_2}+P_{y_9}-P_{y_1}+2P_{z_{10}}-2P_{z_7}],$$
$$|X^2-Y^2\rangle_B{}^a=\alpha d_{x^2-y^2}{}^B-\tfrac{1}{2}(1-\alpha^2)^{1/2}\times[P_{x_2}-P_{x_8}+P_{y_9}-P_{y_1}].$$

Thus using Eq. (B11) for the ξ component, for example, the orbits we use on ion B are the $3\,t_{2g}$ antibonding orbitals, the $|YZ\rangle_B{}^b\,t_{2g}{}^p$ bonding orbital, and the $e_g(\xi)$ antibonding orbital, where,

$$e_g(\xi)=\tfrac{1}{2}\alpha(\sqrt{3}d_{x^2-y^2}{}^B-d_{z^2}{}^B)+\tfrac{1}{2}\sqrt{3}(1-\alpha^2)^{1/2}\times[4P_{x_8}-4P_{x_2}+2P_{y_1}-2P_{y_9}+2P_{z_7}-2P_{z_{10}}].$$

We approximate the exchange between two orbitals as follows:

$$J_{AB}{}^{12}=\int a(1)b(2)H_{\rm ex}{}^{ab}(1,2)b(1)a(2),$$

and if $a=x+y$ and $b=w+v$, which are in the form of molecular orbitals, we can approximate

$$J_{12}{}^{ab}\cong\int x(1)w(2)H_{\rm ex}{}^{ab}(1,2)w(1)x(2)+\int x(1)v(2)H_{\rm ex}{}^{ab}(1,2)v(1)x(2)+\int y(1)w(2)H_{\rm ex}{}^{ab}(1,2)w(1)y(2)+\int y(1)v(2)H_{\rm ex}{}^{ab}(1,2)v(1)y(2).$$

We have neglected terms like

$$\int x(1)w(2)H_{\rm ex}{}^{ab}(1,2)w(1)y(2)$$

and

$$\int x(1)w(2)H_{\rm ex}{}^{ab}(1,2)v(1)y(2),$$

which are an order of magnitude smaller than the ones we are considering because they are one or more orders higher in an overlap integral. We have also limited the interactions to those between d orbitals of the same symmetry, d orbitals and neighboring p orbitals, and p orbitals on the same ligand. We now use these approximations and calculate the *isotropic* exchange energy. We take for the isotropic exchange interaction the sum of interactions between the $|t_{2g}{}^3\,{}^4A_{2g}\rangle$ states on ions A and B; we obtain

$$\Delta E_{\rm iso}=\gamma^4[J_{dxy}{}^A{}_{dxy}{}^B+J_{dxz}{}^A{}_{dxz}{}^B+J_{dyz}{}^A{}_{dyz}{}^B]+\frac{\gamma^2(1-\gamma^2)}{4}\left\{\begin{array}{l}J_{dxy}{}^B{}_{Py_1}+J_{dxy}{}^B{}_{Px_2}+J_{dxy}{}^B{}_{Pz_2}+J_{dxy}{}^B{}_{Pz_1}+J_{dxy}{}^A{}_{Py_2}+J_{dxy}{}^A{}_{Px_1}\\+J_{dxy}{}^A{}_{Pz_1}+J_{dxy}{}^A{}_{Pz_2}+J_{dyz}{}^B{}_{Py_1}+J_{dyz}{}^B{}_{Px_2}+J_{dyz}{}^B{}_{Pz_2}+J_{dyz}{}^B{}_{Pz_1}\\+J_{dyz}{}^A{}_{Py_2}+J_{dyz}{}^A{}_{Px_1}+J_{dyz}{}^A{}_{Pz_1}+J_{dyz}{}^A{}_{Pz_2}+J_{dxz}{}^B{}_{Py_1}+J_{dxz}{}^B{}_{Px_2}\\+J_{dxz}{}^B{}_{Pz_2}+J_{dxz}{}^B{}_{Pz_1}+J_{dxz}{}^A{}_{Py_2}+J_{dxz}{}^A{}_{Px_1}+J_{dxz}{}^A{}_{Pz_1}+J_{dxz}{}^A{}_{Pz_2}\end{array}\right\}+\frac{(1-\gamma^2)^2}{16}\left\{\begin{array}{l}J_{Px_1Py_1}+J_{Px_2Py_2}+J_{Pz_2Py_2}+J_{Pz_1Px_1}+J_{Py_1Pz_1}+J_{Px_2Pz_2}\\+J_{Pz_1Pz_1}+J_{Pz_2Pz_2}\end{array}\right\}. \quad \text{(B15)}$$

We have now arrived at the aforementioned orthogonality problem. How do we interpret terms like $J_{pz_1pz_1}$, $J_{Pz_2Pz_2}$ and (although not quite as obvious) $J_{dyz}{}^B{}_{Pz_1}$? They arise because the molecular orbitals for ion A are not orthogonal to those for ion B. Had we used a set of linear combinations of Wannier functions which had the correct point group symmetry, we probably would have arrived at functions which looked like the molecular orbitals, but which were orthogonal between sites. Unfortunately, at this time, such a method of choosing linear combinations of the Wannier functions does not exist, so that we make do with the molecular orbitals. We know from the work of Anderson[17] that there is a net cost of energy required to make the space part of the wavefunctions on different sites orthogonal. Since the space functions do not need to be orthogonal if the spin functions are orthogonal, the problem does not exist if the two orbitals are coupled antiferromagnetically. Therefore, whenever we encounter an exchange parameter J between nonorthogonal orbitals, we will treat that J as an antiferromagnetic exchange integral.

We set all of the other p-p exchange integrals equal to the Hund's rule exchange on the ligands. The p-d

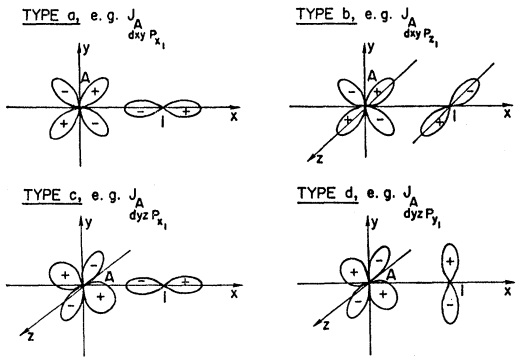

FIG. 9. Classification of ferromagnetic p-d exchange interactions.

exchange integrals are now classified according to order of magnitude by a simple argument. In Fig. 9 we classify the p-d exchange integrals by the type of overlap which exists between the p and d orbitals. We now assume that $J_a \gg J_b \gg J_d$ and $J_c \approx J_b$ because the J_{p-d} exchange of type a (denoted by $J_{p\text{-}d^a}$) has the lobes of both p and d orbits pointing toward the other, while type b and type c have only the lobes of one orbit pointing toward the other. For type d the lobes of both p and d orbits point perpendicular to the vector between them so that $\langle r_{12}\rangle$ is maximized. Implicit in the characterization of the types of exchange is the assumption that the Coulombic term is dominant in the exchange integrals.

We also have antiferromagnetic exchange interactions which arise as a result of the aforementioned nonorthogonality of orbits. An example of such an antiferromagnetic interaction is the exchange integral $J_{dxy\,^4Py_1}$, which we classify as type A. The p and d orbits involved in $J_{dxy\,^4Py_1}$ are shown in Fig. 10. Using these classifications in Eq. (B15) we get

$$\begin{aligned}\Delta E_{\rm iso}=&\gamma^4[J_{dxy\,^4dxy^B}+J_{dyz\,^4dyz^B}+J_{dxz\,^4dxz^B}]\\&+\tfrac{1}{4}\gamma^2(1-\gamma^2)\{7J_{p\text{-}d^a}+5J_{p\text{-}d^b}+3J_{p\text{-}d^c}+5J_{p\text{-}d^d}\\&+4J_{p\text{-}d^A}\}+\tfrac{3}{8}(1-\gamma^2)^2J_{p\text{-}p}+\tfrac{1}{8}(1-\gamma^2)^2J_{p\text{-}p^A},\end{aligned}\quad\text{(B16)}$$

where $J_{p\text{-}p^A}$ represents an antiferromagnetic p-p exchange term such as $J_{Px_1Pz_1}$. We now proceed to calculate the *anisotropic* exchange energy, which involves the exchange interaction between the components of the $t_{2g}{}^p$ unpaired spin and the $(t_{2g})^3$ configuration on ion A, plus the interaction between components of the e_g orbital on ion B and the $(t_{2g})^3$ configuration on ion A. We first calculate the exchange interaction between the

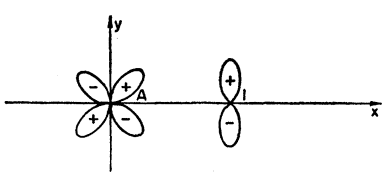

FIG. 10. An antiferromagnetic p-d exchange interaction.

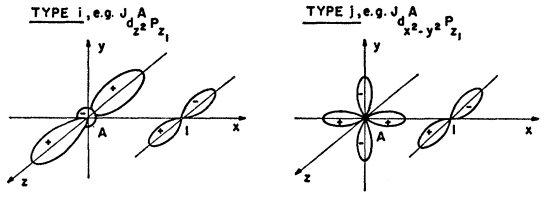

FIG. 11. Ferromagnetic p-d exchange interactions.

$(t_{2g})^3$ configuration on ion A and the particular combination $[2t_{2g}{}^p(\zeta)-t_{2g}{}^p(\xi)-t_{2g}{}^p(\eta)]$ of the components of the $t_{2g}{}^p$ unpaired spin on ion B. We get the following result:

$$\begin{aligned}&J_{AB}(2t_{2g}{}^p(\zeta)-t_{2g}{}^p(\xi)-t_{2g}{}^p(\eta))\\&=\gamma^2(1-\beta^2)[2J_{dxy\,^4dxy^B}-J_{dyz\,^4dyz^B}-J_{dxz\,^4dxz^B}]\\&+\tfrac{3}{8}(1-\gamma^2)\beta^2J_{p\text{-}p}-\tfrac{1}{8}(1-\gamma^2)\beta^2J_{p\text{-}p^A}\\&+\tfrac{1}{4}\gamma^2\beta^2[8J_{p\text{-}d^a}+4J_{p\text{-}d^c}-2pJ_{p\text{-}d^b}-2J_{p\text{-}d^d}-2J_{p\text{-}d^A}].\end{aligned}\quad\text{(B17)}$$

Before writing down the exchange interaction between the e_g orbital on B and $|(t_{2g})^3\,{}^4A_{2g}\rangle$ state of A, we need to define four more types of interactions. (See Figs. 11 and 12.) Clearly both i and j are ferromagnetic and $J_i \approx J_d$, while $J_j \approx J_b$. Both type A_1 and type A_2 represent antiferromagnetic exchange interactions and it appears that $J_{p\text{-}d^{A_1}} > J_{p\text{-}d^{A_2}}$. Using these classifications we calculate in Eq. (B18) the exchange interaction between ion A in state $|{}^4A_{2g}\rangle$ and the specific combination of components of the e_g orbitals given by $[2e_g(\zeta)-e_g(\xi)-e_g(\eta)]$.

$$\begin{aligned}&J_{AB}(2e_g(\zeta)-e_g(\zeta)-e_g(\eta))\\&=-\tfrac{1}{8}(1-\gamma^2)(1-\alpha^2)J_{p\text{-}p}-\tfrac{1}{8}(1-\gamma^2)(1-\alpha^2)J_{p\text{-}p^A}\\&+\tfrac{1}{4}\alpha^2(1-\gamma^2)[3J_{p\text{-}d^{A_2}}-3J_{p\text{-}d^{A_1}}+3J_{p\text{-}d^i}-3J_{p\text{-}d^j}]\\&\quad-\tfrac{1}{4}\gamma^2(1-\alpha^2)[2J_{p\text{-}d^A}+2J_{p\text{-}d^b}+2J_{p\text{-}d^d}].\end{aligned}\quad\text{(B18)}$$

In order to use Eq. (B10) to get the anisotropy energy contribution from a particular state, we need to convert the J_{AB} to $J_{AB}{}'$ using Eq. (B9). Thus we need to calculate λ and $({}^4A_{2g}\|T_{1g}\|{}^4T_{2g})$. In order to derive the spin Hamiltonian we defined λ by Eq. (B2).

$$\langle g|H_{\rm so}|n\rangle=\lambda\sum_{i=x,y,z}S_i\langle g|L_i|n\rangle.$$

For states $|n\rangle$ representing two-ion states with ion A in a

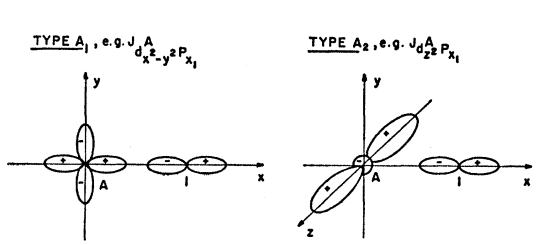

FIG. 12. Antiferromagnetic p-d exchange interactions.

$|{}^4A_{2g}\rangle$ state and ion B in a $|{}^4T_{2g},\gamma\rangle$ state we can write

$$\langle g|H_{so}|n\rangle=\langle {}^4A_{2g}|H_{so}|{}^4T_{2g}\rangle=\lambda\sum_i S_i\langle {}^4A_{2g}|L_i|\ {}^4T_{2g}\rangle.$$

Both of the single-ion matrix elements have been calculated in Appendix A for the $|({}^5E)\ {}^4T_{2g}\rangle$ state. Using the expressions calculated there we obtain

$$\tfrac{3}{4}i[2\alpha(1-\beta^2)^{1/2}\zeta_d+\beta(1-\alpha^2)^{1/2}\zeta_I]$$
$$=\lambda S\{-\tfrac{1}{2}i\sqrt{5}[2\alpha(1-\beta^2)^{1/2}+\beta(1-\alpha^2)^{1/2}]\}.$$

Thus for $S=\frac{3}{2}$ (and since $\zeta_I\gg\zeta_d$) we get

$$\lambda\cong-(1/\sqrt{5})\zeta_I, \text{ provided that we take}$$
$$-\tfrac{1}{2}i\sqrt{5}\beta(1-\alpha^2)^{1/2} \text{ for } \langle {}^4A_{2g}|L_i|\ {}^4T_{2g}\rangle. \quad \text{(B19)}$$

Thus for the $|({}^5E)\ {}^4T_{2g}\rangle$ state of configuration (b) we obtain

$$\Delta E_{\text{aniso}}=\frac{27}{15}\times\frac{1}{5}\times\left(\frac{\zeta_I}{U({}^5E)}\right)^2\left[\frac{15}{4}\beta^2(1-\alpha^2)\right]$$
$$\times\{J_{AB}(2e_g(\zeta)-e_g(\xi)-e_g(\eta)) \quad \text{(B20)}$$
$$-\tfrac{1}{4}J_{AB}(2t_{2g}{}^p(\zeta)-t_{2g}{}^p(\xi)-t_{2g}{}^p(\eta))\}$$
$$\cong 0.015\{J_{AB}(e_g)-\tfrac{1}{4}J_{AB}(t_{2g}{}^p)\},$$

where we are using the same estimates for covalency, spin orbit, and transfer energies that were used in Appendix A for the g-value calculation. Note that for the state $|({}^3E)\ {}^4T_{2g}\rangle$ we get minus the expression above, but $U({}^3E)\approx 2U({}^5E)$ so that the anisotropy energy from the $|({}^3E)\ {}^4T_{2g}\rangle$ state is about $-\frac{1}{4}$ that from the $|({}^5E)\ {}^4T_{2g}\rangle$ state.

Writing out (B20),

$$\Delta E_{\text{aniso}}\cong 0.015\left\{\begin{array}{l}-\frac{1}{8}(1-\gamma^2)[(1-\alpha^2)+\frac{3}{4}\beta^2]J_{p\text{-}p}-\frac{1}{8}(1-\gamma^2)[(1-\alpha^2)-\frac{1}{4}\beta^2]J_{p\text{-}p}{}^A+\frac{3}{4}\alpha^2(1-\gamma^2)\\ \times[J_{p\text{-}d}{}^{A_2}-J_{p\text{-}d}{}^{A_1}]+\frac{1}{2}\gamma^2[\frac{1}{4}\beta^2-(1-\alpha^2)]J_{p\text{-}d}{}^A-\frac{1}{2}\gamma^2\beta^2J_{p\text{-}d}{}^a-\frac{3}{4}\alpha^2(1-\gamma^2)J_{p\text{-}d}{}^j\\ -\frac{1}{2}\gamma^2\{[(1-\alpha^2)-\frac{1}{4}\beta^2]J_{p\text{-}d}{}^b+\frac{1}{2}\beta^2J_{p\text{-}d}{}^c\}+\frac{3}{4}\alpha^2(1-\gamma^2)J_{p\text{-}d}{}^i-\frac{1}{2}\gamma^2[(1-\alpha^2)-\frac{1}{4}\beta^2]J_{p\text{-}d}{}^d\end{array}\right\}. \quad \text{(B21)}$$

We have assumed the $J_{d\,{}^4d^B}$ terms approximately cancel in Eq. (B14). Using the order-of-magnitude estimates we made for the different types of exchange and assuming the antiferromagnetic parts just about cancel since $1-\alpha^2\approx\frac{1}{4}\beta^2$, we arrive at the following approximation for ΔE_{aniso}

$$\Delta E_{\text{aniso}}\cong 0.015\{-0.005J_{p\text{-}p}-0.5J_{p\text{-}d}{}^a\}. \quad \text{(B22)}$$

Likewise approximating ΔE_{iso} from Eq. (B16) we get

$$\Delta E_{\text{iso}}\cong 0.01\{7J_{p\text{-}d}{}^a\}+0.0006J_{p\text{-}p}+0.0002J_{p\text{-}p}{}^A$$
$$+0.01\{4J_{p\text{-}d}{}^A\}+3J_{d\,{}^4d^B}. \quad \text{(B23)}$$

From the fact that the total isotropic exchange is ferromagnetic with an exchange constant of 14 cm^{-1}, we know that ΔE_{iso} favors the ferromagnetic state by $6J\cong 6\times 14\ \text{cm}^{-1}=84\ \text{cm}^{-1}$. Therefore,

$$|0.07J_{p\text{-}d}{}^a+0.0006J_{p\text{-}p}|\cong 84\ \text{cm}^{-1}$$
$$+|0.04J_{p\text{-}d}{}^A+0.0002J_{p\text{-}p}{}^A+3J_{d\,{}^4d^B}|.$$

($J_{d\,{}^4d^B}$ is the Anderson[18] kinetic exchange term and can be either ferromagnetic or antiferromagnetic, but is probably small.) If we assume $J_{p\text{-}p}\cong 20\,000\ \text{cm}^{-1}$ and $J_{p\text{-}d}{}^a\cong\frac{1}{10}J_{p\text{-}p}$ we get

$$152\ \text{cm}^{-1}\approx 84\ \text{cm}^{-1}+84\ \text{cm}^{-1} \text{ (if } J_{p\text{-}d}{}^A\cong J_{p\text{-}d}{}^a),$$

which is reasonable if the d_Ad_B exchange is small. Using these numbers we calculate that

$$\frac{\Delta E_{\text{aniso}}}{\Delta E_{\text{iso}}}\cong -0.015\frac{\{0.005+0.05\}J_{p\text{-}p}}{\frac{1}{2}\{0.0006+0.007\}J_{p\text{-}p}}\cong -0.217. \quad \text{(B24)}$$

We must reduce this by 25% due to the $|({}^3E){}^4T_{2g}\rangle$ state and, therefore, for these two states we have

$$\Delta E_{\text{aniso}}/\Delta E_{\text{iso}}\cong -0.16. \quad \text{(B25)}$$

It must be stressed at this point that the sign and the order of magnitude of the effect are the only really significant things in these calculations, since we have used quite a few numerical estimates. Since the isotropic exchange is ferromagnetic, the exchange integral is negative and, therefore, the anisotropy energy is positive. That is, the $|3,3\rangle$ state is higher in energy than the $|3,0\rangle$ state.

If the entire calculation is repeated for the $|{}^4T_{2g}\rangle$ states arising from configuration (c) given in Appendix A, we find that the contribution to the anisotropy of exchange is an order of magnitude smaller than the contribution that we have just calculated for configuration (b).

[18] P. W. Anderson, Phys. Rev. **115**, 2 (1959).